The Meteoritical Society

Meteoritics & Planetary Science 48, Nr 8, 1383–1400 (2013)
doi: 10.1111/maps.12141

^{26}Al-^{26}Mg isotope systematics of the first solids in the early solar system

Noriko T. KITA[1*], Qing-Zhu YIN[2], Glenn J. MACPHERSON[3], Takayuki USHIKUBO[1], Benjamin JACOBSEN[4], Kazuhide NAGASHIMA[5], Erika KURAHASHI[6], Alexander N. KROT[5], and Stein B. JACOBSEN[7]

[1]WiscSIMS, Department of Geoscience, University of Wisconsin-Madison, Madison, Wisconsin 53706, USA
[2]Department of Geology, University of California, Davis, California 95616, USA
[3]Department of Mineral Sciences, MRC-119, U.S. National Museum of Natural History, Smithsonian Institution, Washington, District of Columbia 20560, USA
[4]Lawrence Livermore National Laboratory, Livermore, California 94551, USA
[5]Hawai'i Institute of Geophysics and Planetology, School of Ocean, Earth Science and Technology, University of Hawai'i at Mānoa, Honolulu, Hawai'i 96822, USA
[6]Institut für Mineralogie, Westfälische Wilhelms-Universität Münster, Münster 48149, Germany
[7]Department of Earth and Planetary Science, Harvard University, Cambridge, Massachusetts 02138, USA
[*]Corresponding author. E-mail: noriko@geology.wisc.edu

(Received 21 May 2012; revision accepted 11 May 2013)

Abstract–High-precision bulk aluminum-magnesium isotope measurements of calcium-aluminum-rich inclusions (CAIs) from CV carbonaceous chondrites in several laboratories define a bulk ^{26}Al-^{26}Mg isochron with an inferred initial ^{26}Al/^{27}Al ratio of approximately 5.25×10^{-5}, named the canonical ratio. Nonigneous CV CAIs yield well-defined internal ^{26}Al-^{26}Mg isochrons consistent with the canonical value. These observations indicate that the canonical ^{26}Al/^{27}Al ratio records initial Al/Mg fractionation by evaporation and condensation in the CV CAI-forming region. The internal isochrons of igneous CV CAIs show a range of inferred initial ^{26}Al/^{27}Al ratios, $(4.2–5.2) \times 10^{-5}$, indicating that CAI melting continued for at least 0.2 Ma after formation of their precursors. A similar range of initial ^{26}Al/^{27}Al ratios is also obtained from the internal isochrons of many CAIs (igneous and nonigneous) in other groups of carbonaceous chondrites. Some CAIs and refractory grains (corundum and hibonite) from unmetamorphosed or weakly metamorphosed chondrites, including CVs, are significantly depleted in ^{26}Al. At least some of these refractory objects may have formed prior to injection of ^{26}Al into the protosolar molecular cloud and its subsequent homogenization in the protoplanetary disk. Bulk aluminum and magnesium-isotope measurements of various types of chondrites plot along the bulk CV CAI isochron, suggesting homogeneous distribution of ^{26}Al and magnesium isotopes in the protoplanetary disk after an epoch of CAI formation. The inferred initial ^{26}Al/^{27}Al ratios of chondrules indicate that most chondrules formed 1–3 Ma after CAIs with the canonical ^{26}Al/^{27}Al ratio.

INTRODUCTION

Calcium-aluminum-rich inclusions (CAIs) in CV (Vigarano type) carbonaceous chondrites have the oldest measured Pb-Pb ages of any early solar system objects (Amelin et al. 2002, 2010; Bouvier and Wadhwa 2010; Bouvier et al. 2011b; Connelly et al. 2012). The mineralogy and major element chemistry of CAIs are generally similar to those expected for solids in equilibrium with a high-temperature ($T > 1300$ K) gas of solar composition (e.g., Grossman 1972; but see Grossman et al. [2000] for a discussion of the differences). Amoeboid olivine aggregates (AOAs) are mostly loose aggregates of olivine that enclose small

CAIs. The oxygen-isotope ratios of CAIs and AOAs are enriched in ^{16}O by approximately 50‰ compared to the terrestrial mantle (e.g., Clayton et al. 1973; Yurimoto et al. 2008) and are similar to those of the Sun inferred from the analyses of solar wind returned by the GENESIS spacecraft (McKeegan et al. 2011). CAIs also contain excess ^{10}B from the in situ decay of the short-lived radionuclide ^{10}Be, which might form largely by solar energetic particle irradiation at the time of CAI formation (e.g., McKeegan et al. 2000; MacPherson et al. 2003; Wielandt et al. 2012). The above observations collectively indicate that CAIs and AOAs formed from a gas of approximately solar composition in the hot (ambient temperature > 1300 K) innermost region of the protoplanetary disk at the birth of the solar system, and subsequently were transported to outer disk regions (e.g., Shu et al. 1996; Ciesla 2010). In contrast, the petrologic, chemical, and isotopic characteristics of chondrules indicate that they formed by transient heating events in the dust-enriched and relatively cold (ambient temperature < 650 K) regions of the protoplanetary disk (e.g., Connolly and Love 1998; Alexander et al. 2008). Absolute U-Pb chronology (Amelin et al. 2010) and relative ^{26}Al-^{26}Mg chronology of chondrules (e.g., Kita et al. 2000; Kurahashi et al. 2008a; Villeneuve et al. 2009) both indicate that most chondrules solidified 2–3 million years (Ma) after CAIs, although some chondrules appear to have formed contemporaneously with CAIs (e.g., Yin et al. 2009; Connelly et al. 2012).

MacPherson et al. (1995) suggested that, on a large scale, ^{26}Al was distributed homogeneously in the early solar system although grain-to-grain heterogeneities clearly existed. More recent studies are consistent with this conclusion (Kita et al. 2005; Krot et al. 2009; Villeneuve et al. 2009). If the assumption that ^{26}Al was homogeneous in the early solar system is correct, the ^{26}Al-^{26}Mg system provides the highest time-resolution among the short-lived radionuclide chronometers due to the short half-life of ^{26}Al, 0.705 Ma (Norris et al. 1983). Here, we summarize recent results on the inferred initial $^{26}Al/^{27}Al$ ratios in CAIs, AOAs, and chondrules based on the high-precision magnesium isotope measurements using multicollector secondary ion mass spectrometry (MC-SIMS) and multicollector inductively coupled plasma mass spectrometry (MC-ICP-MS). The relative ages of CAIs, AOAs, and chondrules inferred from the ^{26}Al-^{26}Mg chronometer thus provide important constraints on the models of the solar protoplanetary disk evolution (e.g., Ciesla 2010; Cuzzi et al. 2010). This article is focused primarily on recent high-precision CAI and AOA data; the chondrule data were discussed thoroughly in two recent review papers (Krot et al. 2009; Kita and Ushikubo 2012).

INITIAL $^{26}AL/^{27}AL$ RATIO IN THE PROTOPLANETARY DISK

MacPherson et al. (1995) showed that the initial $^{26}Al/^{27}Al$ ratio, denoted herein as $(^{26}Al/^{27}Al)_0$, in most CAIs was approximately 5×10^{-5}. This value, commonly referred to as the "canonical" ratio, is considered to represent the initial $^{26}Al/^{27}Al$ ratio of the solar system. Recently, this ratio has been re-evaluated using high-precision MC-ICP-MS measurements of bulk CAIs from CV carbonaceous chondrites. The first such studies (Bizzarro et al. 2004, 2005; Thrane et al. 2006) gave results that were inconsistent with each other, including the report of so-called supracanonical $(^{26}Al/^{27}Al)_0$ values significantly greater than 5×10^{-5} (Thrane et al. 2006). After improved calibration of mass spectrometric analysis of $^{27}Al/^{24}Mg$ ratios, B. Jacobsen et al. (2008) analyzed 6 Allende CAIs and reported $(^{26}Al/^{27}Al)_0$ of $(5.23 \pm 0.13) \times 10^{-5}$ (Fig. 1a). Baker (2008) and S. B. Jacobsen et al. (2008) also reported similar value to that of B. Jacobsen et al. (2008). Most recently, Larsen et al. (2011) reported $(^{26}Al/^{27}Al)_0$ of $(5.25 \pm 0.02) \times 10^{-5}$ from 5 bulk CAIs and 5 bulk AOAs from the reduced CV chondrite Efremovka (Fig. 1b). Thus, the initial $^{26}Al/^{27}Al$ ratio inferred from bulk CV CAIs is precisely and consistently defined as approximately 5.25×10^{-5} by multiple laboratories.

In all of the studies cited above, the bulk CAI isochron data were obtained from diverse types of CV CAIs, including both nonmelted (primitive) and melted (reprocessed) inclusions. Collectively, these CAIs as a group show a wide range of mass-dependent fractionation of magnesium isotopes, with $\delta^{25}Mg$ ranging from −4‰ to +12‰. The inference is that these CAIs experienced various types of high-temperature events, such as nonequilibrium condensation of refractory solids from gas and kinetically controlled evaporation of refractory melts. The fact that such diverse CAIs (and CAI histories) define a single coherent trend on the bulk ^{26}Al-^{26}Mg isochron diagrams indicates that the initial and principal aluminum-magnesium fractionation, i.e., the original formation of CV CAIs or their precursors by evaporation and condensation processes, occurred within a short period of time, ≤20 ka (Thrane et al. 2006; B. Jacobsen et al. 2008). High-precision internal CAI isochrons indicate that the primitive, unmelted CAIs tend to have values of $(^{26}Al/^{27}Al)_0$ close to 5.2×10^{-5}, consistent with the bulk CAI isochrons, whereas melted and otherwise heavily reprocessed CAIs give a range of values (MacPherson et al. 2010, 2012). Thus, although primitive CAIs and CAI precursors formed over a very short time, reprocessing continued over at least another 0.2 Ma.

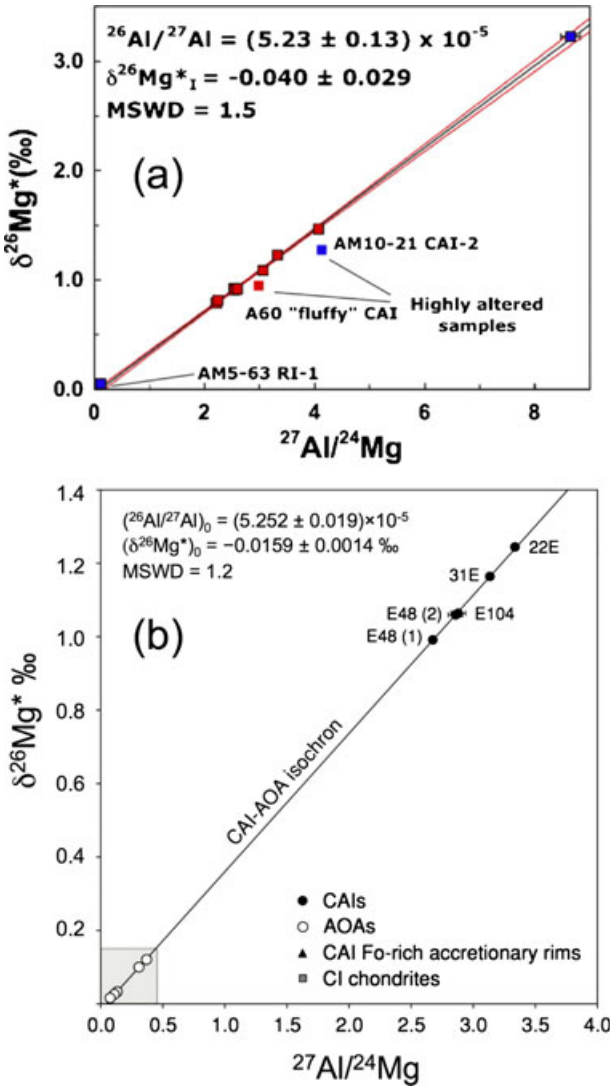

Fig. 1. The ^{26}Al-^{26}Mg isochron of bulk CAIs from CV chondrites. a) Bulk Allende CAI isochron from B. Jacobsen et al. (2008). By defining the excess ^{26}Mg ($\delta^{26}Mg^*$) to be the deviation of ($^{26}Mg/^{24}Mg$) ratio from the terrestrial reference line in parts per thousand (‰), $(^{26}Al/^{27}Al)_0$ is estimated from the slope of the Al-Mg isochron regression with the equation; $\delta^{26}Mg^* = (\delta^{26}Mg^*)_0 + (^{26}Al/^{27}Al)_0 \times (^{27}Al/^{24}Mg) \times 10^3/(^{26}Mg/^{24}Mg)_{DSM3}$, where $(\delta^{26}Mg^*)_0$ is the intercept of the isochron regression line (see Appendix). Two altered CAIs that are off the regression line were not included for isochron regression. b) Bulk Efremovka CAI-AOA isochron by Larsen et al. (2011). The unit of *Y*-axis is converted to $\delta^{26}Mg^*$ (‰) from $\mu^{26}Mg^*$ (ppm) in the original figure.

One of the consequences of the large improvements in analytical precision over the past 10 yr or so is that fine details of the correction procedure now matter relative to the precision of the data. A lively debate has arisen over the form of the equation to be used for correction of intrinsic mass-dependent isotopic fractionation. Equally debated is the value of the fractionation coefficient, β. A detailed discussion of these issues is given in the Appendix.

VARIATIONS IN $^{26}AL/^{27}AL$ RATIOS AMONG CAIS

CAIs from CV Chondrites

Many CV CAIs experienced one or more reheating events in the solar nebula that resulted in, e.g., melting, solid-state recrystallization, and back reactions between the solids and the surrounding gas (e.g., MacPherson and Davis 1993; Hsu et al. 2000). Thus, the internal ^{26}Al-^{26}Mg isochron of any individual inclusion dates the time of last crystallization provided that the magnesium isotopes in the CAI were internally homogenized (i.e., complete resetting of the ^{26}Al-^{26}Mg system), which may or may not have been at the time of original CAI precursor formation. Less extreme secondary reprocessing, whether in the nebula or on the CV parent body, commonly did not reset the ^{26}Al-^{26}Mg system and the observed result is disturbed isochrons. In such cases, the inferred initial $(^{26}Al/^{27}Al)_0$ at the time of those events may or may not be determined accurately. For example, Podosek et al. (1991) reported disturbed isochrons in some Allende CAIs that experienced only incomplete melting or solid-state recrystallization, and these did not give clear $(^{26}Al/^{27}Al)_0$ values. Conversely, MacPherson et al. (2012) analyzed a complex CAI from Vigarano that preserved relicts of the premelted CAI and in this case, both the relicts and the host (melted) CAI individually gave isochrons, which are well resolved from each other. The difference in slope between the two corresponds to a difference in time of formation of about 0.6 Ma.

The large differences in Al/Mg ratios among the major mineral phases in CAIs mean in principle that internal isochrons of individual CAIs can be very tightly constrained. In type A CAIs, melilite ($Ca_2Al_2SiO_7$-$Ca_2MgSi_2O_7$ solid solution) is Al-rich and has high $^{27}Al/^{24}Mg$ ratios of 10–100, whereas pyroxene ($CaMgSi_2O_6$-$CaAl_2SiO_6$-$CaTi^{4+}Al_2O_6$-$CaTi^{3+}AlSiO_6$ solid solution) and spinel ($MgAl_2O_4$) show lower $^{27}Al/^{24}Mg$ ratios of less than ≤5 and approximately 2.6, respectively. Fine-grained spinel-rich CAIs (e.g., Fig. 2a) also contain aluminum-rich melilite, but their grain sizes require SIMS spot sizes ≤5 μm to obtain a full range of $^{27}Al/^{24}Mg$ ratios (Fig. 3; MacPherson et al. 2012). In the pyroxene-rich type B CAIs (Fig. 2b), melilite is more magnesium-rich than in type As, and anorthite ($CaAl_2Si_2O_8$) shows the highest $^{27}Al/^{24}Mg$ ratios of 200–400 (Fig. 4a). Again, pyroxene and spinel show lower $^{27}Al/^{24}Mg$ ratios (Fig. 4b). Type B CAIs are sufficiently coarse-grained that 20–30 μm spot sizes are

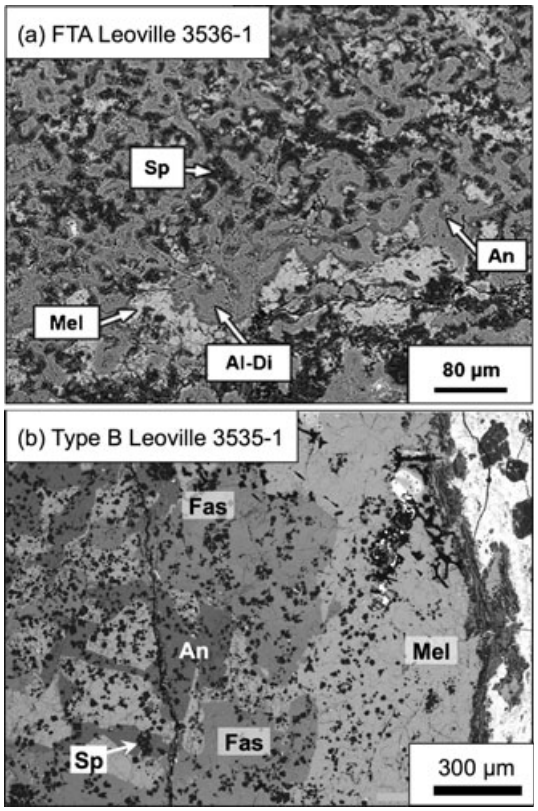

Fig. 2. Examples of unmelted and melted CAIs. (a) Leoville 3536-1 (fine-grained spinel-rich inclusion) is an aggregate of fine-grained (≤5 μm) minerals that never experienced melting (MacPherson et al. 2010). (b) Leoville 3535-1 type B CAI consists of coarse-grained (≥100 μm) minerals that were crystallized from melt (Kita et al. 2012). Mineral phases: "An"- anorthite, "Al-Di"-aluminum-rich diopside, "Fas"-fassaite, "Mel"-melilite, and "Sp"-spinel.

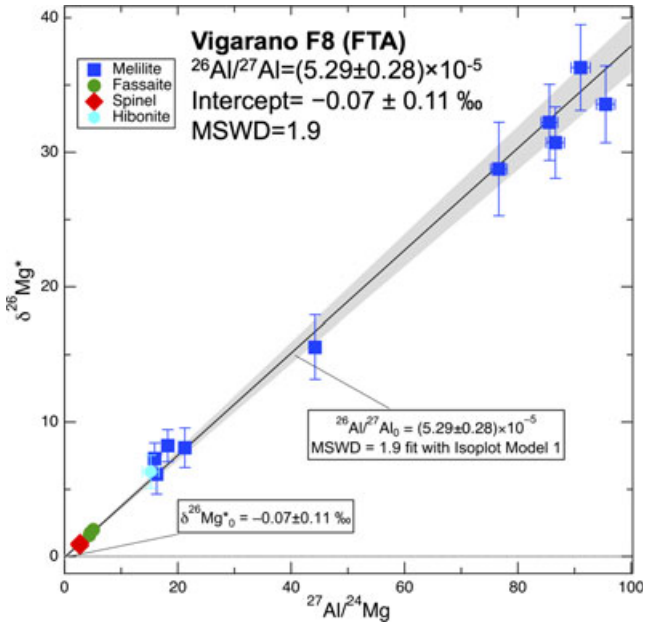

Fig. 3. Internal isochron of unmelted CAI, Vigarano F8 FTA (MacPherson et al. 2012). Melilite data show excess $\delta^{26}Mg^*$ up to approximately 35‰ and the data from multiple phases, including melilite, fassaite, spinel, and hibonite, define well correlated isochron diagram. The $(^{26}Al/^{27}Al)_0$ agrees with that of bulk CAI isochron within analytical uncertainties.

possible during SIMS analysis (Kita et al. 2012). The analyses of mineral separates using solution ICP-MS are possible for large type B CAIs (e.g., B. Jacobsen et al. 2008).

High-precision internal ^{26}Al-^{26}Mg isochrons obtained from different types of CV CAIs (B. Jacobsen et al. 2008; MacPherson et al. 2010, 2012; Bouvier and Wadhwa 2010; Kita et al. 2012) are summarized in Fig. 5. For comparison purposes, it should be noted that in most of these studies, the magnesium-isotope ratios were corrected for mass-dependent fractionation using $\beta = 0.514$ as inferred from the evaporation experiments of a CAI composition melt (Davis et al. 2005). However, B. Jacobsen et al. (2008) used $\beta = 0.511$. The critical point is that the slopes of isochrons are not significantly affected by using one or the other of these two β values (see Table 1A; and also fig. 4 of Wasserburg et al. 2012). Most of these CAIs show a relatively narrow range of $(^{26}Al/^{27}Al)_0$, (4.2–5.3) × 10^{-5}. As reported by MacPherson et al. (2012) based on the ^{26}Al-^{26}Mg analyses of six Vigarano CAIs, there are systematic differences between melted and unmelted CAIs. Unmelted refractory inclusions in Fig. 5 include one FTA, a fine-grained spinel-rich inclusion, and one AOA. The FTA and the fine-grained inclusion, Vigarano 3138-F8 (labeled F8 on Fig. 5) and Leoville 3536-1, show $(^{26}Al/^{27}Al)_0$ of (5.27 ± 0.17) × 10^{-5} and (5.29 ± 0.28) × 10^{-5} (MacPherson et al. 2010, 2012), respectively, that are indistinguishable from those of the bulk CV CAI isochron (B. Jacobsen et al. 2008; Larsen et al. 2011). An amoeboid olivine aggregate from Vigarano (Vig 3138-F5, labeled F5 on Fig. 5) yields $(^{26}Al/^{27}Al)_0$ = (5.13 ± 0.10) × 10^{-5} (MacPherson et al. 2012), which is marginally lower than that of bulk CV CAIs reported by Larsen et al. (2011). These data indicate that the solidification of the most primitive (unmelted) CAIs occurred within a very short time, ≤50 ka, after the initial aluminum–magnesium fractionation event recorded by the bulk CV CAI isochron (Fig. 5).

Melted CAIs represented in Fig. 5 include compact type As (CTAs), type Bs, and one type C (pyroxene-anorthite-rich) CAI. The two CTAs from Vigarano, Vig 3138-F6 and Vig 3138-F9, show distinct $(^{26}Al/^{27}Al)_0$ values of (4.2 ± 0.4) × 10^{-5} and (5.2 ± 0.3) × 10^{-5}, respectively (MacPherson et al. 2012). Six type B CAIs were analyzed using MC-ICP-MS analyses of mineral separates (B. Jacobsen et al. 2008; Bouvier and

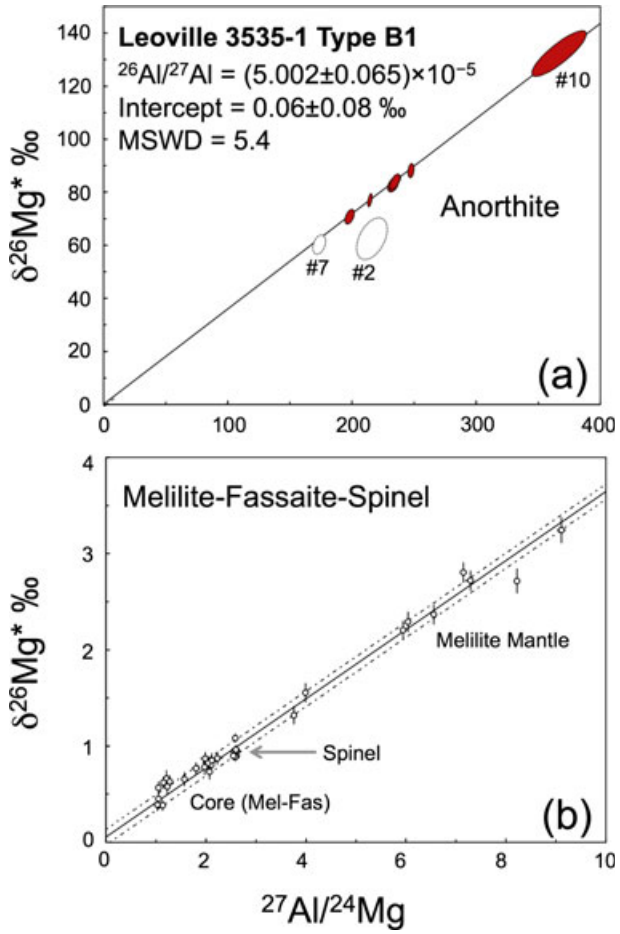

Fig. 4. Internal isochron of melted CAI, Leoville 3535-1 type B CAI (Kita et al. 2012). a) Isochron was regressed through multiple mineral phases. Anorthite data show excess $\delta^{26}Mg^*$ up to 130‰ with well-correlated isochron. b) Expanded view near the origin of the isochron, showing melilite, spinel, and fassaite data. The $(^{26}Al/^{27}Al)_0$ value is slightly lower than that of bulk CAI isochron.

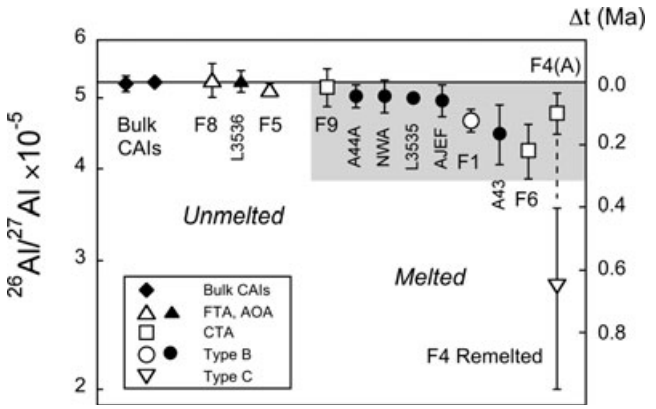

Fig. 5. The $(^{26}Al/^{27}Al)_0$ values of CAIs from CV chondrites including both bulk isochron and internal isochron (after MacPherson et al. 2012). Data sources: B. Jacobsen et al. (2008); Bouvier and Wadhwa (2010); Larsen et al. (2011); Kita et al. (2012); MacPherson et al. (2012). Open symbols are data reported in MacPherson et al. (2012) and filled symbols are from other literatures. Unmelted CAIs (FTAs and AOA) older than melted CAIs. Most CAIs formed and reprocessed within approximately 0.2 Ma, except for one type C CAI (F4) that experienced melting approximately 0.7 Ma later.

Wadhwa 2010) and high-precision MC-SIMS analyses (Kita et al. 2012; MacPherson et al. 2012). They show a narrow range of variations in $(^{26}Al/^{27}Al)_0$ of (4.5–5.0) $\times$ 10^{-5}, with four of them clustering at approximately 5.0 $\times$ 10^{-5}. MacPherson et al. (2012) also reported a compound type C CAI (Vig 3138-F4) that consists of a relict type A region surrounded by type B and type C mantles, sequentially. They obtained $(^{26}Al/^{27}Al)_0 = (4.8 \pm 0.3) \times 10^{-5}$ for the relict type A, while the type C region yielded a ratio of $(2.8 \pm 0.8) \times 10^{-5}$ that is significantly lower than that of other CAIs. Collectively, most CV CAIs were reprocessed within 0.2 Ma of their primary formation, but the reprocessing of some CV CAIs continued for nearly approximately 1 Ma, possibly in regions where chondrules were being formed (MacPherson et al. 2012).

MacPherson et al. (2012) also showed a magnesium-isotope evolution diagram, following the work of Villeneuve et al. (2009) that compares the intercepts of the ^{26}Al-^{26}Mg isochron $((\delta^{26}Mg^*)_0)$ of each CAI with its respective $(^{26}Al/^{27}Al)_0$. Most of their CAI data are consistent with closed system evolution since the establishment of the bulk CAI isochron at $^{26}Al/^{27}Al = 5.25 \times 10^{-5}$. This observation indicates that the elemental Al/Mg fractionation of bulk CAIs occurred very early at the formation of their precursors, and not at the time of later reheating events.

CAIs from CR and CO Chondrites and Acfer 094

CAIs in CR and CO chondrites, and Acfer 094 (ungrouped carbonaceous chondrite) are less abundant and smaller than those in CVs, but mineralogically, more pristine in the sense that they have undergone less secondary alteration and reprocessing. Previous ^{26}Al-^{26}Mg studies of CAIs from these chondrites generally showed results consistent with the canonical $^{26}Al/^{27}Al$ ratio (e.g., Russell et al. 1998; Sugiura and Krot 2007). Here, we summarize the most recent, high-precision, recent internal isochron studies of CAIs from CRs, CO3s, and Acfer 094.

Makide et al. (2009) reported internal isochrons for seven CAIs from CRs and found $(^{26}Al/^{27}Al)_0$ in the range (4.4–5.4) $\times$ 10^{-5}, consistent with the results for most CV CAIs. Ushikubo et al. (2011) reported preliminary SIMS internal isochron data for six CAIs from Y-81020 (CO3) and Acfer 094. These CAIs

include FTAs, melilite-rich, and anorthite-rich varieties, and show a range of $(^{26}Al/^{27}Al)_0$ values (4–5) $\times 10^{-5}$ again similar to those in CV CAIs, indicating that they formed within the first 0.2 Ma after primary Al/Mg fractionation. One anorthite-rich CAI from Acfer 094 has an exceptionally low $(^{26}Al/^{27}Al)_0$ value of $(5.4 \pm 0.5) \times 10^{-6}$, which is similar to those of chondrules in the same meteorite (Ushikubo et al. 2013). This may represent reprocessing in the solar nebula gas much later than the original formation of the precursor CAI, analogous to the type C CAI (Vigarano 3138-F4) described above. An alternative model requires formation of the CAI prior to injection and homogenization of ^{26}Al in the protoplanetary disk, but the anorthite-rich character of such CAIs (less refractory than anorthite-poor varieties) argues against such a model.

CAIs and Refractory Grains Depleted in ^{26}Al

Numerous CAIs and refractory grains have been analyzed that show little or no evidence for former ^{26}Al being present. Some of these can be attributed to later reprocessing that reset the isotopic system (e.g., MacPherson et al. 1995). However, late-stage *formation* of some of the ^{26}Al-poor CAIs is unlikely, because they also contain endemic stable isotope anomalies in a variety of elements (Ca, Ti, Ba, others) that are of nucleosynthetic origin (Sahijpal and Goswami 1998). The latter include FUN (fractionation and unidentified nuclear effects) CAIs (Wasserburg et al. 1977), and platy hibonite crystals (PLACs; e.g., Ireland 1988). The reason why FUN CAIs and related objects are so deficient in ^{26}Al remains unexplained.

Recently, a third group of ^{26}Al-deficient objects has been identified. It includes some of the micron-sized corundum grains; corundum-bearing, grossite-rich, and hibonite-rich CAIs; and most CAIs from CH carbonaceous chondrites (Weber et al. 1995; Sugiura and Krot 2007; Krot et al. 2008, 2012; Liu et al. 2009, 2012; Makide et al. 2009, 2011; Hsu et al. 2011). These refractory objects show ^{16}O-rich isotope signature and the ^{10}B excesses from the decay of ^{10}Be at the level similar to CAIs with the canonical $^{26}Al/^{27}Al$ ratio, indicating that ^{26}Al-poor and ^{26}Al-rich CAIs formed in similar environments. Furthermore, according to the low $(\delta^{26}Mg^*)_0$ intercepts of the ^{26}Al-^{26}Mg isochrons, the ^{26}Mg deficits have been reported in some ^{26}Al-poor CAIs (Liu et al. 2009; Makide et al. 2009) and one type B CAI with the canonical $^{26}Al/^{27}Al$ ratio (Wasserburg et al. 2012). These observations indicate that stable isotope and ^{26}Al heterogeneities existed among CAIs. Considering that most CAIs show a narrow range of $(^{26}Al/^{27}Al)_0$ close to the canonical value, ^{26}Al-depleted CAIs may have formed earlier than other CAIs, prior to injection and homogenization of ^{26}Al in the early solar system (e.g., Sahijpal and Goswami 1998; Boss et al. 2008; Gritschneder et al. 2012; see more discussion in Krot et al. 2012), or represent minor groups of CAIs that formed in localized heterogeneous isotope reservoirs.

VARIATIONS IN INITIAL $^{26}AL/^{27}AL$ RATIOS AMONG CHONDRULES

The initial $^{26}Al/^{27}Al$ ratios inferred from internal isochrons of chondrules in the least metamorphosed chondrites (type 3.0) mostly are in the range of (0.5–1) $\times 10^{-5}$, which corresponds to 2–3 Ma after formation of CAIs with canonical $(^{26}Al/^{27}Al)_0$ (e.g., Kita et al. 2000; Kunihiro et al. 2004; Kurahashi et al. 2008a; Villeneuve et al. 2009; Ushikubo et al. 2013). An exception is chondrules from CR chondrites. Only a few CR chondrules show resolvable ^{26}Mg excesses ($\delta^{26}Mg^* > 0$) with inferred $(^{26}Al/^{27}Al)_0$ that are similar to those in chondrules from other chondrite groups. Most other CR chondrules show no resolvable excess ^{26}Mg ($\delta^{26}Mg^* \leq 0$), with an upper limit on the $(^{26}Al/^{27}Al)_0$ values of $<3 \times 10^{-6}$ (Nagashima et al. 2007, 2008; Kurahashi et al. 2008b; Hutcheon et al. 2009). These data are summarized in Fig. 6.

In the recent review of Al-Mg data from chondrules in type 3.0 chondrites, Kita and Ushikubo (2012) showed that chondrules from a single chondrite group typically have a narrow range of $(^{26}Al/^{27}Al)_0$. For example, type I chondrules in Y-81020 and Acfer 094 and those of type II chondrules in Semarkona (LL3.0) show the average $(^{26}Al/^{27}Al)_0$ values of $(7.0 \pm 1.6) \times 10^{-6}$ (1SD, $n = 14$; Kurahashi et al. 2008a), $(5.7 \pm 1.6) \times 10^{-6}$ (1SD, $n = 9$; Ushikubo et al. 2013), and $(7.0 \pm 1.8) \times 10^{-6}$ (1SD, $n = 4$; Kita et al. 2000), respectively. Although the $(^{26}Al/^{27}Al)_0$ values in a single meteorite are variable and correspond to the time difference of as long as approximately 1 Ma, most chondrules in LL3s, CO3s, and Acfer 094 formed within a narrow time scale, much shorter than a million years. These restricted ages for chondrules in each chondrite suggest that radial transport of chondrules must have been limited (Cuzzi et al. 2010) such that they may also preserve the group-specific chemical and isotopic characters among chondrules in a single chondrite group (Scott and Krot 2005).

TIME SCALE OF PROTOPLANETARY DISK EVOLUTION

The ^{26}Al-^{26}Mg systems of CAIs and chondrules potentially can test models for the evolution of protoplanetary disk in our solar system. The differences

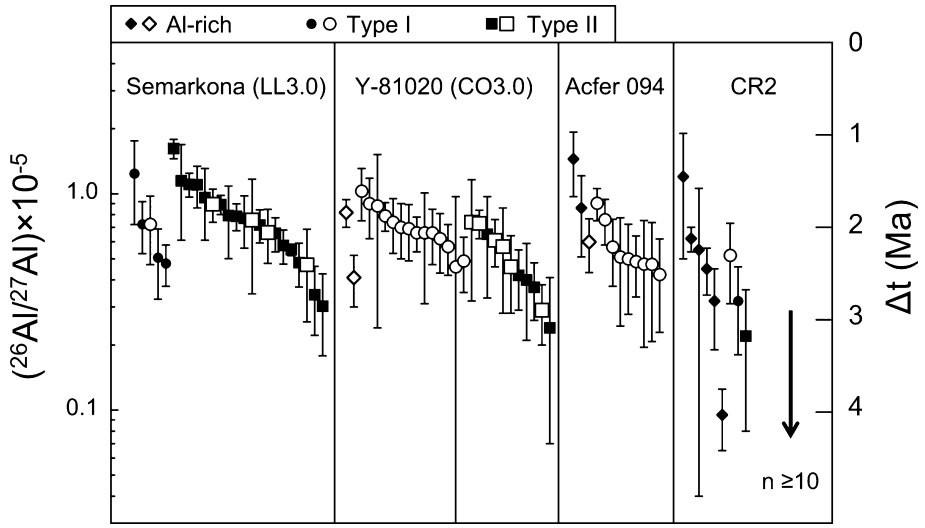

Fig. 6. Compilation of the initial $^{26}Al/^{27}Al$ ratios inferred from internal isochron regressions of ^{26}Al-^{26}Mg data for chondrules from primitive chondrites (after Kita and Ushikubo [2012]; reference therein). Error bars shown are 2 SE from isochron regression. Data from type 3.0 chondrites are shown except for those in CR chondrites. Open larger symbols are those from Kita et al. (2000), Kurahashi et al. (2008a), and Ushikubo et al. (2013) that used 3–5 μm small SIMS spots with long counting time (typically 3–8 h per spot). Data from other literatures are shown as smaller filled symbols.

in initial $^{26}Al/^{27}Al$ values among diverse kinds of objects, relative to the bulk CAI initial value $(^{26}Al/^{27}Al)_0 = (5.25 \pm 0.02) \times 10^{-5}$, are (with the usual assumptions) a clock of early solar system events relative to time zero (formation of the first solids). These events can in turn be compared with the lifetime of individual evolutional stages of young stellar objects (YSOs). We note, however, "time zero" from the ^{26}Al chronology may not be the exact time of the birth of the solar system when the protosolar molecular cloud started to collapse. As indicated from ^{26}Al-depleted refractory inclusions and minerals, the initial molecular cloud of our solar system would be either heterogeneous or depleted in ^{26}Al. Thus, solid precursors of CV CAIs might not form at the beginning of collapse stage from the cloud with homogeneously distributed ^{26}Al. The relative time scales inferred from YSOs and the ^{26}Al chronology of CAIs would be biased, depending on the timing when bulk Al-Mg isochron of CV CAIs was established.

According to the spectral energy distribution (SED), YSOs are classified into five stages (classes 0/I/Flat/II/III) that reflect condition of infalling clouds and circumstellar disks (Table 1). Classes 0 and I are embedded protostars, in which central stars actively form by collapse of a parental molecular cloud core. Gas and dust in the cloud (or envelope) accrete to a circumstellar disk due to rotation of the cloud, and the star accretes mass from the disk. Class II YSOs correspond to classical T Tauri stars (CTTS), which are surrounded by an accretion disk consisting of dust and gas. YSOs with flat infrared spectrums are transitional between classes I and II, and accretion from the envelope onto the protostar may still be occurring. Class III YSOs correspond to weak-lined T Tauri stars (WTTS) without a dusty disk, probably due to planetary growth. Evans et al. (2009) estimated the lifetimes of individual classes of YSOs, based on *Spitzer* surveys in multiple large molecular clouds, as shown in Table 1. They assumed the lifetime of class II YSOs to be 2 ± 1 Ma, and then estimated those of other classes based on the relative populations. This resulted in lifetimes of 0.1, 0.44, and 0.35 Ma, for classes 0, I, and Flat SED, respectively.

It is generally thought that CAIs formed in the earliest stages of disk evolution (class 0 and I) of our own solar system, when temperatures of the inner disk increased above >1500 K due to a high accretion rate of the disk ($>10^{-6}$ $M_\odot$ yr^{-1}; Boss 1998). Prior to the work of Evans et al. (2009), estimates of the lifetimes of class 0 and I stages were orders of 0.01 and 0.1 Ma, respectively (Greene et al. 1994; Feigelson and Montmerle 1999). This seemed consistent with the narrow range of $(^{26}Al/^{27}Al)_0$ among normal CAIs. However, using the new estimates by Evans et al. (2009), the combined lifetime of classes 0 and I YSOs (approximately 0.5 Ma) and transition period from class I to II (Flat SED approximately 0.4 Ma) are much longer than relative time difference among normal CAIs (≤0.2 Ma). One explanation for the discrepancy may relate to outward transport processes in the inner solar system. Ciesla (2010) argued that

Table 1. Evolution of young stellar objects (after Williams and Cieza 2011).

Class	0	I	Flat	II	III
Physical properties[a]	$M_C > M_S > M_D$	$M_S > M_C \sim M_D$		$M_D \sim 0.01\ M_S$	$M_D \ll 0.01\ M_S$
Lifetime[b] (Ma)	0.10	0.44	0.35	2 ± 1	
Age[c] (Ma)	0.1	0.5	0.9	3	<10

[a]Comparison of masses of central star (M_S), molecular cloud core (M_C), and circumstellar disk (M_D).
[b]Median lifetime of Evans et al. (2009) that assumes class II lifetime of 2 ± 1 Ma.
[c]Cumulative ages using lifetime of individual classes.

formation of refractory solids could have continued for as long as approximately 1 Ma in the inner regions of the disk, but the CAIs that are preserved in meteorites are those that formed during the first 0.1 Ma, after the end of infall when outward radial transport was most efficient. Yang and Ciesla (2012) further examined the transport of refractory solids in the protoplanetary disk during and after the infall of molecular cloud, in which they assumed that the infall period lasted 0.3 Ma. They suggested that CAIs surviving in asteroidal regions of a 2 Ma-old disk would be dominated by the population around the time that infall stopped. Both models seem to be consistent with the narrow range of relative ages (≤0.2 Ma) observed among CAIs, while the infall stages of the young Sun would have been longer (≥0.5 Ma).

Eisner et al. (2005) found that the accretion rates of the inner disk of class I YSOs are significantly lower than infall rates of cloud. It implies that the disk masses are high and gravitationally unstable, which would result in enhanced episodic accretion, such as FU Orionis outbursts (e.g., Hartmann and Kenyon 1996). Boss et al. (2012) performed the numerical calculations of the evolution of a marginally gravitationally unstable disk to simulate the FU Orionis phenomenon. They suggested that most CAIs formed at the end of the FU Orionis outburst phases and mainly represent only a last few bursts. The model also explains the narrow range of $(^{26}Al/^{27}Al)_0$ among normal CAIs, because refractory solids, possibly with lower $(^{26}Al/^{27}Al)_0$, that formed during earlier bursts may have not survived during the later bursts. Primary formation of CV CAIs might have occurred during such a single FU Orionis event and subsequent reheating events occurred mainly within 0.2 Ma when the ^{26}Al-^{26}Mg systems in CAIs were internally reset. It is possible that these large CAIs were concentrated in a specific area of the disk due to radial transport (e.g., Ciesla 2010), where the CV chondrite parent body formed.

Outward radial transport in class I YSOs would have been greater in the earliest period than later time (e.g., Yang and Ciesla 2012), which may transfer earliest formed fine-grained refractory objects to outer disk including comet-forming regions. This mechanism may explain the existence of ^{26}Al-depleted CAIs with large nucleosynthetic isotope anomalies if the molecular cloud accreted to the solar system was initially heterogeneous in isotope ratios and depleted in ^{26}Al (see Krot et al. 2012). These anomalous CAIs would have been transported to the outer solar system quickly and escaped from later major heating events that produced majority of normal CAIs.

Chondrule formation appears to have occurred in the cold ($T < 650$ K), dust-rich regions of the disk, possibly near its mid-plane of class II disk. In class II YSOs, accretion rate of the disk would be reduced to approximately $10^{-8}\ M_\odot\ yr^{-1}$, so that temperature exceeded >1300 K only at the inner edge of the disk. The lifetime of class II YSOs is generally considered approximately 2 Ma, which seems to be compatible to the Al-Mg ages of chondrules relative to the time of CAI formation.

UNRESOLVED PROBLEMS

Initial $^{26}Mg/^{24}Mg$ of the Bulk CAI Isochron

On a ^{26}Al-^{26}Mg isochron diagram for an individual CAI, the intercept of the isochron with the vertical axis gives the value of initial $^{26}Mg/^{24}Mg$ in the CAI at the time of formation. The intercept will evolve (increase) for individual CAIs that experience remelting or other secondary resetting, and higher values will reflect more recent crystallization ages (e.g., MacPherson et al. 2012). On an isochron diagram defined by a suite of bulk CAIs formed at approximately the same time, the intercept of the whole-CAI isochron with the vertical axis gives the value of initial $^{26}Mg/^{24}Mg$ in the reservoir at the time of CAI formation. This initial bulk solar system $^{26}Mg/^{24}Mg$ ratio also evolved with time from its initial value as ^{26}Al decayed, until the ^{26}Al was effectively gone after several million years (e.g., Villeneuve et al. 2009). The initial $^{26}Mg/^{24}Mg$ ratio expressed as $(\delta^{26}Mg^*)_0$ of the solar system is expected to be approximately −0.038‰ lower than the value today, assuming homogeneous initial magnesium isotope ratios, homogeneous initial aluminum isotope ratios

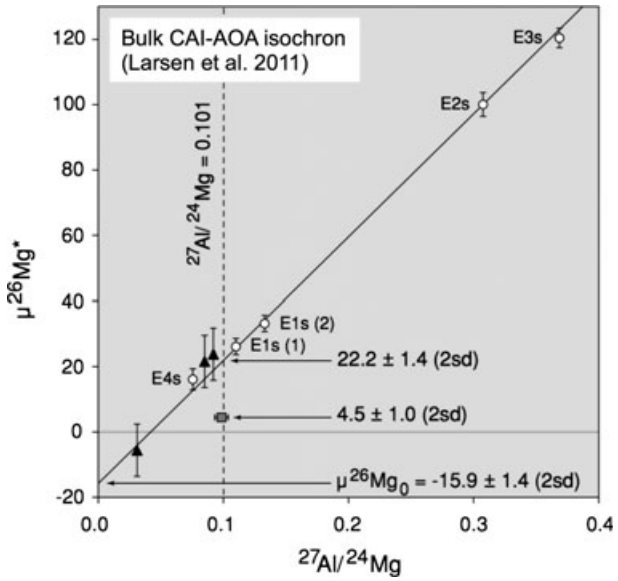

Fig. 7. Intercept of bulk CAI-AOA Al-Mg isochron (Larsen et al. 2011). The figure corresponds to the shaded area in Fig. 1b. The *Y*-axis is shown as a unit of $\mu^{26}Mg^*$ (ppm), which is equivalent to $\delta^{26}Mg^*(‰) \times 1000$. Open circles—bulk AOAs, filled triangles—forsterite-rich accretionary rims of CAIs, gray square—bulk CI chondrites.

($^{26}Al/^{27}Al = 5.25 \times 10^{-5}$), and a bulk solar system ratio of $^{27}Al/^{24}Mg = 0.101$ as defined by CI chondrites (Palme and Jones 2003). If CV CAIs formed from an isotope reservoir identical to the average solar system, the isochron intercept for these CAIs should also be −0.038‰. B. Jacobsen et al. (2008) obtained a bulk CAI isochron and determined the intercept to be $(\delta^{26}Mg^*)_0 = -0.040 \pm 0.029‰$, which is consistent with the predicted value. However, the uncertainty of the intercept is relatively large because bulk CAIs show $^{27}Al/^{24}Mg$ ratios larger than 2, requiring a significant extrapolation to the *y*-axis. Larsen et al. (2011) determined a more precise intercept for a bulk CAI isochron, $(\delta^{26}Mg^*)_0 = -0.016 \pm 0.002‰$, by including bulk AOA data with low $^{27}Al/^{24}Mg$ ratios (0.1–0.4) for the regression (Fig. 7). This intercept is significantly higher than the predicted solar system initial $(\delta^{26}Mg^*)_0$, but it is largely constrained by the AOA data. Unfortunately, the use of bulk AOA data together with bulk CAI data to construct an isochron is justified only if the Al/Mg ratios of bulk CAIs and bulk AOAs were fractionated at the same time from the same isotope reservoir, and their bulk ^{26}Al-^{26}Mg system subsequently remained closed. Wasserburg et al. (2012) showed that these AOA data of Larsen et al. (2011) in fact plot above the bulk CAI isochron, indicating that the AOAs must postdate the bulk CAIs. Wasserburg et al. (2012) further showed that regression of only the CAI data (i.e., without the AOAs) yields $(\delta^{26}Mg)_0 = -0.030 \pm 0.040‰$, entirely consistent with the value $(\delta^{26}Mg^*)_0 = -0.040 \pm 0.029‰$ determined by B. Jacobsen et al. (2008). The question thus arises whether AOAs should legitimately be considered together with CAIs in determining $(\delta^{26}Mg)_0$.

Because AOAs contain refractory minerals such as spinel and aluminous diopside, and also possess ^{16}O-rich signatures similar to those of CAIs, it is generally considered that AOAs formed by condensation from a solar nebula gas, but at somewhat lower temperature than did CAI precursors s (e.g., Krot et al. 2004). An internal isochron for one AOA, Vigarano 3138-F5, does yield a marginally lower $(^{26}Al/^{27}Al)_0$ than that of bulk CAIs (MacPherson et al. 2012), but it is risky to conclude from this one object that AOAs in general formed later than did CAIs, especially as it is now clear that many CAIs experienced remelting over a period of at least 0.2 Ma after initial CAI formation (MacPherson et al. 2012). Indeed, textures such as 120° triple grain junctions in some AOAs themselves indicate reprocessing (annealing, and possibly even incipient melting) subsequent to their initial formation (Komatsu et al. 2001). Nevertheless, we agree with Wasserburg et al. (2012) that caution should be taken in using low Al/Mg AOAs together with other bulk CAIs to define solar system initial $^{26}Mg/^{24}Mg$ ratio, because the resulting elevated initial $^{26}Mg/^{24}Mg$ ratio is highly dependent on the AOAs whose temporal relation with CAIs is so uncertain.

Degree of Heterogeneity of ^{26}Al in the Protoplanetary Disk

Even taking into account the existence of CAIs that clearly had little or no ^{26}Al at the time of their initial formation, the balance of evidence indicates that at a very early time, the protoplanetary disk became sufficiently homogenized such that the extent of local heterogeneity in $^{26}Al/^{27}Al$ was on the order of ±10% at most. The relative Al-Mg ages obtained from various meteoritic samples, which include CAIs, chondrules, and various achondrites, are broadly consistent with those obtained from Pb-Pb, ^{53}Mn-^{53}Cr, and ^{182}Hf-^{182}W systems (e.g., Nyquist et al. 2009; Amelin et al. 2010; Bouvier and Wadhwa 2010; Bouvier et al. 2011a, 2011b). In Fig. 8, relative ages of CAIs and various igneous meteorites obtained from multiple chronometers are compared, by using quenched angrites as an age anchor (D'Orbigny and Sahara 99555, with Al-Mg ages of 4.7 ± 0.2 and 4.7 ± 0.4 Ma later than the time defined by the bulk CAI isochron, respectively; Spivak-Birndorf et al. 2009). As shown in Fig. 8a, relative Al-Mg and Mn-Cr ages of three achondrites from

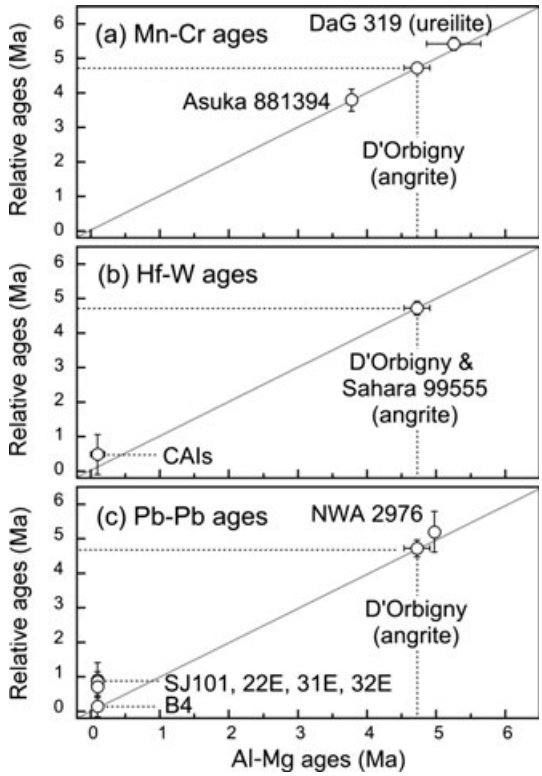

Fig. 8. Comparison of Al-Mg ages of CAIs and igneous meteorites with their (a) Mn-Cr, (b) Hf-W, and (c) Pb-Pb ages. The Al-Mg ages are shown as time after bulk CAI isochron with $(^{26}Al/^{27}Al)_0 = 5.25 \times 10^{-5}$ (Larsen et al. 2011). Other ages are anchored by quenched angrite (D'Orbigny and Sahara 99555) by applying $(^{26}Al/^{27}Al)_0 = (5.06 \pm 0.92) \times 10^{-7}$ (D'Orbigny; Spivak-Birndorf et al. 2009), $(^{53}Mn/^{55}Mn)_0 = (3.24 \pm 0.04) \times 10^{-6}$ (D'Orbigny; Glavin et al. 2004), and $(^{182}Hf/^{180}Hf)_0 = (6.99 \pm 0.11) \times 10^{-5}$ (D'Orbigny and Sahara 99555; Kleine et al. 2012). The Pb-Pb ages are shown relative to D'Orbigny (Amelin 2008), which is corrected for the measured uranium isotope ratios by Brennecka and Wadhwa (2012). Other data are from Burkhardt et al. (2008), Wadhwa et al. (2009a), Amelin et al. (2010), Goodrich et al. (2010), Bouvier et al. (2011a, 2011b), Kleine et al. (2012), and Connelly et al. (2012). The internal Al-Mg ages of CAIs that were measured for Hf-W and Pb-Pb systems are not available, so that they are assumed to be 0.1 Ma with dashed lines extending to approximately 1 Ma on Al-Mg ages.

distinct asteroidal sources show excellent agreements, indicating the homogeneous distribution of ^{26}Al in the asteroidal-forming regions. We note that ^{53}Mn-^{53}Cr system is not applied to CAIs because of nucleosynthetic Cr isotope anomaly (e.g., Nyquist et al. 2009). The Hf-W age difference between CAI (Burkhardt et al. 2008) and the quenched angrites (Kleine et al. 2012) is 4.2 ± 0.6 Ma, which is in agreement with the Al-Mg age of the quenched angrites (Fig. 8b). In Fig. 8c, we compare available Pb-Pb ages of CAIs (Amelin et al. 2010; Bouvier et al. 2011b; Connelly et al. 2012) and achondrites (Amelin 2008; Bouvier et al. 2011a; Brennecka and Wadhwa 2012). Since the variability in uranium isotope ratios ($^{238}U/^{235}U$) among CAIs and meteorite samples has been revealed (e.g., Amelin et al. 2010; Brennecka et al. 2010), high-precision uranium isotope measurements of the individual meteorite samples are required to estimate the accurate Pb-Pb ages (Amelin et al. 2010). Therefore, Pb-Pb age data shown in Fig. 8c are limited to those corrected for the uranium isotope ratios. The relative Pb-Pb ages between several CAIs (Amelin et al. 2010; Connelly et al. 2012) and D'Orbigny (Amelin 2008; Brennecka and Wadhwa 2012) are approximately 3.8 Ma, which is approximately 1 Ma shorter than the Al-Mg age of the quenched angrites. However, Pb-Pb ages of another CAI (B4) and NWA 2976 (ungrouped achondrite) show an age difference consistent with the Al-Mg age of NWA 2976 (Bouvier et al. 2011a, 2011b). We note that the internal Al-Mg isochrons of any of these CAIs are not currently available, which could be used as a test for potential secondary isotope disturbances in the CAIs (e.g., Wadhwa et al. 2009b). In summary, estimates of the age differences between CAIs and other meteorite samples using the Al-Mg and other isotopic chronometers differ by approximately 1 Ma or less. This translates into potential variations in the $^{26}Al/^{27}Al$ ratio of a factor of approximately 2.

Two recent studies address the potential heterogeneity in $^{26}Al/^{27}Al$ and stable magnesium isotopes from the perspective of bulk chondrite analyses, and compare those with the bulk CAI isochron. Schiller et al. (2010) obtained magnesium isotopic data for 18 bulk chondrites that include nearly all groups of chondrites. As shown on a ^{26}Al-^{26}Mg isochron diagram in Fig. 9a, the data define a line that goes through the bulk CV CAI data of B. Jacobsen et al. (2008). From this, the authors concluded that heterogeneities of $^{26}Al/^{27}Al$ and $\delta^{26}Mg^*$ in the protoplanetary disk were less than 30% and 0.005‰, respectively. Larsen et al. (2011) obtained data for nine bulk chondrites (including CI, ordinary, enstatite, and R varieties) and several achondrites with very high precisions. Their bulk chondrite data are entirely consistent with the bulk chondrite data obtained by Schiller et al. (2010) (Fig. 9a). However, instead of a straightforward interpretation of the data that argues in favor of homogeneous distribution of ^{26}Al in the bulk solar system materials, Larsen et al. (2011) suggested two alternative possibilities: (1) a significantly large heterogeneity in ^{26}Al (maximum depletion by 80%, or factor of five) or (2) magnesium isotope heterogeneity in the protoplanetary disk where meteorite parent asteroids formed. Here, we examine the claim made by Larsen et al. (2011) in detail.

The model estimating the initial $^{26}Al/^{27}Al$ ratios of individual chondrite-forming regions that was applied by

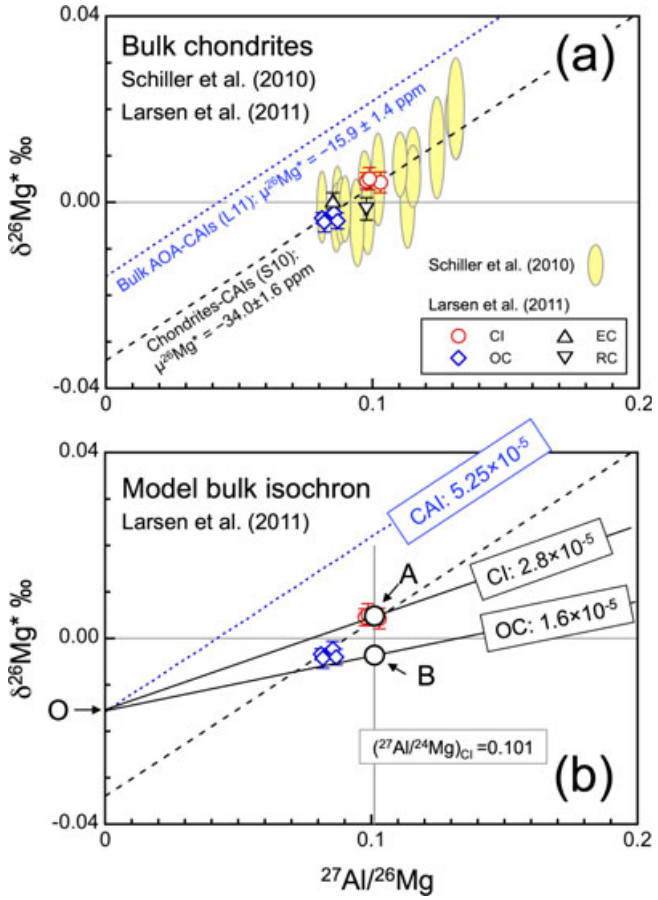

Fig. 9. The ^{26}Al-^{26}Mg system of bulk chondrites. a) Bulk chondrite data from Schiller et al. (2010) and Larsen et al. (2011). Bulk CAI-AOA isochron is from Larsen et al. (2011) with intercept at -15.9 ± 1.4 ppm and the $(^{26}Al/^{27}Al)_0 = (5.25 \pm 0.02) \times 10^{-5}$. Bulk CAI-chondrite isochron is from Schiller et al. (2010) with intercept at -34.0 ± 1.6 ppm and the $(^{26}Al/^{27}Al)_0 = (5.21 \pm 0.06) \times 10^{-5}$, which combined bulk CAI data of B. Jacobsen et al. (2008). b) Model bulk isochron for chondrite reservoirs by Larsen et al. (2011). Points O, A, and B are the intercept of bulk CAI-AOA isochron, bulk CI chondrite data, and bulk ordinary chondrite (OC) data that is horizontally shifted to the CI chondrite ($^{27}Al/^{24}Mg$) ratio, respectively. The model $(^{26}Al/^{27}Al)_0$ of CI and OC reservoirs are estimated from the slopes of lines O-A and O-B, respectively. Although bulk OC data plot on the same isochron with CAIs and CI chondrites, the model $(^{26}Al/^{27}Al)_0$ of OC reservoir is estimated three times lower than that of bulk CAIs. See text for a detailed discussion.

Larsen et al. (2011) is illustrated in Fig. 9b. They assumed the initial δ^{26}Mg* of the solar system to be -0.0159 ± 0.0014‰ according to the bulk CAI-AOA isochron (point "O") and the measured δ^{26}Mg* values of bulk chondrites are the result of additional ^{26}Mg from ^{26}Al decay under the solar ($^{27}Al/^{24}Mg$) ratio (i.e., 0.101 for CI chondrites). For the CI chondrite-forming region, $(^{26}Al/^{27}Al)_0$ of $(2.8 \pm 0.3) \times 10^{-5}$ is estimated from the slopes of the line O-A, where point "A" represents the average value for the bulk CI chondrite data. For the ordinary chondrite-forming region, the initial $^{26}Al/^{27}Al$ ratio of $(1.6 \pm 0.3) \times 10^{-5}$ is estimated from the slopes of the line O-B, where the point "B" represents a point shifted to the right of bulk OC chondrite data to ($^{27}Al/^{24}Mg$) ratio of 0.101. Larsen et al. (2011) applied the same model to enstatite chondrites, angrites, and ureilites with the estimated $^{26}Al/^{27}Al$ ratios down to $(1.1 \pm 0.3) \times 10^{-5}$. As illustrated in Fig. 9b, the Larsen et al. (2011) argument for $^{26}Al/^{27}Al$ heterogeneity is based on the assumption that the entire solar system's $^{26}Mg/^{24}Mg$ isotopic composition is homogenous to the level of ± 0.0014‰ (or 1.4 ppm), which is not justified, given the documented Mg isotopic heterogeneity and the potential pitfalls (discussed above) of using AOAs to help constrain the solar system initial $(\delta^{26}Mg^*)_0$ (e.g., Wasserburg et al. 2012).

Another major problem of the model by Larsen et al. (2011) is that they dismissed the importance of elemental fractionation that could have occurred before the complete decay of ^{26}Al in the solar nebula as well as in the differentiated parent bodies. Most chondritic meteorites show variable enrichments and depletion of refractory elements relative to Mg compared with those of CI chondrites at the level of 10–40% (e.g., Scott and Krot 2003). Igneous differentiation of asteroidal bodies involve formation of basaltic magma and mafic partial-melting residues, which are significantly enriched and depleted in Al_2O_3 relative to MgO. In contrast, the model applied by Larsen et al. (2011) assumes that meteorite samples did not experience any Al/Mg fractionation within the first 5 Ma of the solar system formation, which is incorrect. For example, bulk ordinary chondrites show slightly lower $^{27}Al/^{24}Mg$ ratios (approximately 0.08; Larsen et al. 2011) compared with CI chondrites (approximately 0.10), which are also seen among bulk chondrules (e.g., Kita et al. 2010; Fig. 2). If Al depletion occurred very early (<1 Ma) in the ordinary chondrite-forming regions, the bulk δ^{26}Mg* values of ordinary chondrites would be slightly lower than CI chondrites as seen in data from Larsen et al. (2011). In the case of bulk ureilite data in Larsen et al. (2011), the lowest δ^{26}Mg* value of approximately -0.008‰ was obtained among all the bulk meteorite data (Fig. 10). The bulk ureilites showed the low $^{27}Al/^{24}Mg$ ratios of ≤ 0.01 (10 times lower than that of CI chondrites) because of extensive igneous differentiation and extraction of melt (e.g., Wilson et al. 2008). The low δ^{26}Mg* value of bulk ureilites would likely be the result of early removal of aluminum-rich melt before complete decay of ^{26}Al. A single-stage evolution of bulk ureilites from CI chondritic precursors is illustrated in Fig. 10, providing the inferred $(^{26}Al/^{27}Al)_0$ of approximately 2×10^{-5} at the time of igneous differentiation of the ureilite parent body. Baker

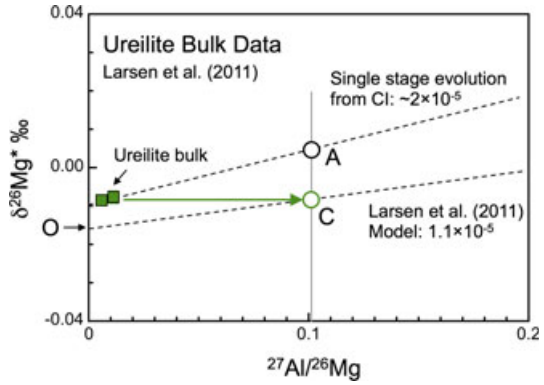

Fig. 10. Bulk aluminum-magnesium isotope measurements of ureilites. Two bulk ureilite data are shown as filled square from Larsen et al. (2011). Point C is the bulk ureilite data that is horizontally shifted to the CI chondrite ($^{27}Al/^{24}Mg$) ratio. The model $(^{26}Al/^{27}Al)_0$ of ureilite parent body was estimated to be $(1.1 \pm 0.3) \times 10^{-5}$ by Larsen et al. (2011), which is illustrated by the line O–C. Alternatively, a single-stage evolution of ureilite from CI chondritic precursor (isochron connecting bulk ureilite data and point A) may indicate that the igneous fractionation of the parent body occurred with $^{26}Al/^{27}Al$ approximately 2×10^{-5}, corresponding to approximately 1 Ma after the time of bulk CAI isochron.

et al. (2012) reported similar deficits in $\delta^{26}Mg^*$ values from pallasites and ureilites, from which they suggested differentiation of their parent bodies within 1–2 Ma after CAI formation. Thus, less radiogenic magnesium isotope in differentiated meteorites might simply reflect differentiation of the parent asteroid that occurred before the complete decay of ^{26}Al, but may not be related to the heterogeneity of ^{26}Al in their precursor regions.

Larsen et al. (2011) compared ^{54}Cr anomaly ($\varepsilon^{54}Cr$) and $\delta^{26}Mg^*$ of bulk meteorites and suggested that the apparent ^{26}Al heterogeneity correlates with stable isotope anomalies of other elements observed among different groups of meteorites (Trinquier et al. 2007). However, Schiller et al. (2010) observed no correlation between $\varepsilon^{54}Cr$ and $\delta^{26}Mg^*$ from 11 different groups of bulk meteorites, so that the suggestion made by Larsen et al. (2011) is not supported when larger groups of meteorite data are considered.

We argue that the data of Larsen et al. (2011) can be interpreted in a simpler and more straightforward manner. CAIs and CI chondrites can be derived from the same isotopic reservoir, with the initial $(^{26}Al/^{27}Al)$ and $\delta^{26}Mg^*$ isotope ratios given by a regression of the bulk CAI plus CI chondrite data from Larsen et al. (2011) as plotted on an Al-Mg isochron diagram. The result of such a regression gives $(^{26}Al/^{27}Al)_0 = (5.33 \pm 0.02) \times 10^{-5}$ and $(\delta^{26}Mg^*)_0 = -0.0335 \pm 0.0012‰$ (MSWD = 0.65), which are close to the bulk chondrite-bulk CAI isochron calculated by Schiller et al. (2010). Some scattering of bulk chondrite data from the CI chondrite–bulk CAI isochron may be a result of chemical fractionation processes such as condensation, evaporation, and chondrule formation, and which probably occurred during a few million years in the protoplanetary disk before ^{26}Al had completely decayed. Ultra high-precision magnesium isotope analyses of bulk meteorites demonstrated by Larsen et al. (2011) are certainly very useful to understand large-scale ^{26}Al-^{26}Mg systematics in the protoplanetary disk. However, the initial ^{26}Al abundance of source regions of individual meteorite parent bodies remains uncertain until the timing and degree of Al/Mg fractionations for components in meteorites are precisely known. As shown in Figs. 9 and 10 collectively, the data seem to strengthen rather than weaken the idea of large-scale ^{26}Al homogeneity of in the protoplanetary disk.

SUMMARY

Bulk CV CAIs yield well-defined ^{26}Al-^{26}Mg whole-rock isochrons with an initial $^{26}A/^{27}Al$ ratio of approximately 5.25×10^{-5}. Internal ^{26}Al-^{26}Mg isochrons of CV CAIs show systematic differences that correlate with their texturally inferred histories, specifically that unmelted CAIs are the oldest and melted CAIs experienced reprocessing over an extended time of up to 0.2 Ma. This time scale from CV CAIs is similar to that indicated from the internal isochron studies of non-CV CAIs. At least some of the CAIs that are ^{26}Al depleted may have formed during earlier events, possibly prior to the injection and homogenization of ^{26}Al in the early solar system. Bulk chondrite magnesium-isotope data are consistent with homogeneous initial ^{26}Al abundance in the protoplanetary disk, in contrast to the recent claim by Larsen et al. (2011).

Future studies need to address the temporal and genetic relationship between CAIs and AOAs, specifically whether they originally formed at the same time from common Al and Mg isotope reservoirs. Additional "ultra-high precision" bulk CAI analyses with a wider range of Al/Mg ratios will help us to evaluate the bulk CAI isochron more precisely without use of AOA data. Coordinated studies of bulk and internal ^{26}Al-^{26}Mg system, U-Pb ages, and stable isotope anomalies on the same CAIs will address the magnitude of ^{26}Al heterogeneity in the earliest solar system.

Recent observations and models of protostar evolutions indicate that inner regions of circumstellar disks might experience several episodic heating events that occurred within the first approximately 0.5 Ma. Detailed isotope records preserved in CAIs would be a key to explore duration of such episodic events, particularly to clarify if most CAIs with narrow ranges

of $(^{26}A/^{27}Al)_0$ formed during one or a few of latest events prior to the end of core collapse stage.

Acknowledgments—The authors acknowledge the organizing committee of the Workshop on "Formation of the First Solid in the Solar System" for the opportunity of this article. The constructive comments by Joel Baker and James Connelly and the careful handling by associate editor Edward Scott improved clarity of the manuscript significantly. This work is supported by NASA programs (NNX09AB88G, NK; NNX11AJ51G, QZY; NNX11AD43G, GJM; NNX11 AK82G, SBJ; NNX10AH76G, ANK) and UC Laboratory Fees Research Program 12_LR-237921 to QZY.

Editorial Handling—Dr. Edward Scott

REFERENCES

Alexander C. M. O'D., Grossman J. N., Ebel D. S., and Ciesla F. J. 2008. The formation conditions of chondrules and chondrites. *Science* 320:1617–1619.

Amelin Y. 2008. U-Pb ages of angrites. *Geochimica et Cosmochimica Acta* 72:221–232.

Amelin Y., Krot A. N., Hutcheon I. D., and Ulyanov A. A. 2002. Lead isotopic ages of chondrules and calcium-aluminum-rich inclusions. *Science* 297:1678–1683.

Amelin Y., Kaltenbach A., Iizuka T., Stirling C. G., Ireland T. R., Petaev M., and Jacobsen S. B. 2010. U-Pb chronology of the solar system's oldest solids with variable $^{238}U/^{235}U$. *Earth and Planetary Science Letters* 300:343–350.

Baker J. A. 2008. High-precision ^{26}Al-^{26}Mg dating solid and planetesimal formation in the young solar system. *Geochimica et Cosmochimica Acta Supplement* 72:A45.

Baker J. A., Schiller M., and Bizzarro M. 2012. ^{26}Al-^{26}Mg deficit dating ultramafic meteorites and silicate planetesimal differentiation in the early solar system? *Geochimica et Cosmochimica Acta* 77:415–431.

Bizzarro M., Baker J. A., and Haack H. 2004. Mg isotope evidence for contemporaneous formation of chondrules and refractory inclusions. *Nature* 431:275–278.

Bizzarro M., Baker J. A., and Haack H. 2005. Corrigendum: Mg isotope evidence for contemporaneous formation of chondrules and refractory inclusions. *Nature* 435:1280.

Boss A. P. 1998. Temperature in protoplanetary disks. *Annual Review of Earth and Planetary Sciences* 26:53–80.

Boss A. P., Ipatov S. I., Keiser S. A., Myhill E. A., and Vanhala H. A. T. 2008. Simultaneous triggered collapse of the presolar dense cloud core and injection of short-lived radioisotopes by a supernova shock wave. *The Astrophysical Journal* 686:L119–L122.

Boss A. P., Alexander C. M. O'D., and Podolak M. 2012. Cosmochemical consequences of particle trajectories during FU Orionis outbursts by the early Sun. *Earth and Planetary Science Letters* 345–348:18–26.

Bouvier A. and Wadhwa M. 2010. The age of the solar system redefined by the oldest Pb-Pb age of a meteoritic inclusion. *Nature Geoscience* 3:637–641.

Bouvier A., Spivak-Birndorf L. J., Brennecka G. A., and Wadhwa M. 2011a. New constraints on early solar system chronology from Al-Mg and U-Pb isotope systematics in the unique basaltic achondrite Northwest Africa 2976. *Geochimica et Cosmochimica Acta* 75:5310–5323.

Bouvier A., Brennecka G. A., and Wadhwa M. 2011b. Absolute chronology of the first solids in the solar system (abstract #9054). Workshop on formation of the first solids in the solar system. November 7–9, 2011, Kauai, Hawai'i. LPI Contribution No. 1639.

Brennecka G. A and Wadhwa M. 2012. Uranium isotope compositions of the basaltic angrite meteorites and the chronological implications for the early solar system. *Proceedings of the National Academy of Sciences* 109:9299–9303.

Brennecka G. A, Weyer S., Wadhwa M., Janney P. E., Zipfel J., and Anbar A. D. 2010. $^{238}U/^{235}U$ variations in meteorites: Extant ^{247}Cm and implications for Pb-Pb dating. *Science* 327:449–451.

Burkhardt C., Kleine T., Palme H., Bourdon B., Zipfel J., Friedrich J., and Ebel D. 2008. Hf–W mineral isochron for Ca, Al-rich inclusions: Age of the solar system and the timing of core formation in planetesimals. *Geochimica et Cosmochimica Acta* 72:6177–6197.

Catanzaro E. J., Murphy T. J., Garner E. L., and Shields W. R. 1966. Absolute isotopic abundance ratios and atomic weights of magnesium. *Journal of Resource of the National Bureau of Standards* 70a:453–458.

Ciesla F. J. 2010. The distributions and ages of refractory objects in the solar nebula. *Icarus* 208:455–467.

Clayton R. N., Grossman L., and Mayeda T. K. 1973. Component of primitive nuclear composition in carbonaceous meteorites. *Science* 182:485–488.

Connolly H. C. and Love S. G. 1998. The formation of chondrules: Petrologic tests of the shock wave model. *Science* 280:62–67.

Connelly J. N., Bizzarro M., Krot A. N., Nordlund Å., Wielandt D., and Ivanova M. A. 2012. The absolute chronology and thermal processing of solids in the solar protoplanetary disk. *Science* 338:651–655.

Cuzzi J. N., Hogan R. C., and Bottke W. F. 2010. Towards initial mass functions for asteroids and Kuiper Belt objects. *Icarus* 208:518–538.

Davis A. M., Richter F. M., Mendybaev R. A., Janney P. E., Wadhwa M., and McKeegan K. D. 2005. Isotopic mass fractionation laws and the initial solar system $^{26}Al/^{27}Al$ ratio (abstract #2334). 36th Lunar and Planetary Science Conference. CD-ROM.

Eisner J. A., Hillenbrand L. A., Carpenter J. M., and Wolf S. 2005. Constraining the evolutionary stage of Class I protostars: Multiwavelength observations and modeling. *The Astrophysical Journal* 635:396–421.

Evans N. J., II, Dunham M. M., Jørgensen J. K., Enoch M. L., Merín B., van Dishoeck E. F., Alcalá J. M., Myers P. C., Stapelfeldt K. R., Huard T. L., Allen L. E., Harvey P. M., van Kempen T., Blake G. A., Koerner D. W., Mundy L. G., Padgett D. L., and Sargent A. I. 2009. The *Spitzer* c2d Legacy results: Star-formation rates and efficiencies; evolution and lifetimes. *The Astrophysical Journal Supplement Series* 181:321–350.

Feigelson E. D. and Montmerle T. 1999. High-energy processes in young stellar objects. *Annual Review of Astronomy and Astrophysics* 37:363–408.

Galy A., Yoffe O., Janney P. E., Williams R. W., Cloquet C., Alard O., Halicz L., Wadhwa M., Hutcheon I. D., Ramon E., and Carignan J. 2003. Magnesium isotope heterogeneity

of the isotopic standard SRM980 and new reference materials for magnesium–isotope-ratio measurements. *Journal of Analytical Atomic Spectrometry* 18:1352–1356.

Glavin D. P., Kubny A., Jagoutz E., and Lugmair G. W. 2004. Mn-Cr isotope systematics of the D'Orbigny angrite. *Meteoritics & Planetary Science* 39:693–700.

Goodrich C. A., Hutcheon I. D., Kita N. T., Huss G. R., Cohen B. A., and Keil K. 2010. ^{53}Mn-^{53}Cr and ^{26}Al-^{26}Mg ages of a feldspathic lithology in polymict ureilites. *Earth and Planetary Science Letters* 295:531–540.

Greene T. P., Wilking B. A., André P., Young E. T., and Lada C. J. 1994. Further mid-infrared study of the ρ Ophiuchi cloud young stellar population: Luminosities and masses of pre-main-sequence stars. *The Astrophysical Journal* 434:614–626.

Gritschneder M., Lin D. N. C., Murray S. D., Yin Q.-Z., and Gong M.-N. 2012. The supernova triggered formation and enrichment of our solar system. *The Astrophysical Journal* 745:22 (12pp).

Grossman L. 1972. Condensation in the primitive solar nebula. *Geochimica et Cosmochimica Acta* 36:597–619.

Grossman L., Ebel D. S., Simon S. B., Davis A. M., Richter F. M., and Parsad P. M. 2000. Major element chemical and isotopic compositions of refractory inclusions in C3 chondrites: The separate roles of condensation and evaporation. *Geochimica et Cosmochimica Acta* 64:2879–2894.

Hartmann L. and Kenyon S. J. 1996. The FU Orionis phenomenon. *Annual Review of Astronomy and Astrophysics* 34:207–240.

Hsu W., Wasserburg G. J., and Huss G. R. 2000. High time resolution by use of the ^{26}Al chronometer in the multistage formation of a CAI. *Earth and Planetary Science Letters* 182:15–29.

Hsu W., Guan Y., and Wang Y. 2011. Al-Mg systematics of hibonite-bearing Ca,Al-rich inclusions from Ningqiang. *Meteoritics & Planetary Science* 46:719–728.

Hutcheon I. D., Marhas K. K., Krot A. N., Goswami J. N., and Jones R. H. 2009. ^{26}Al in plagioclase-rich chondrules in carbonaceous chondrites: Evidence for an extended duration of chondrule formation. *Geochimica et Cosmochimica Acta* 73:5080–5099.

Ireland T. R. 1988. Correlated morphological, chemical, and isotopic characteristics of hibonites from the Murchison carbonaceous chondrite. *Geochimica et Cosmochimica Acta* 52:2827–2839.

Jacobsen B., Yin Q.-Z., Moynier F., Amelin Y., Krot A. N., Nagashima K., Hutcheon I. D., and Palme H. 2008. ^{26}Al-^{26}Mg and ^{207} Pb-^{206} Pb systematics of Allende CAIs: Canonical solar initial ^{26}Al/^{27}Al ratio reinstated. *Earth and Planetary Science Letters* 272:353–364.

Jacobsen S. B., Chakrabarti R., Ranen M. C., and Petaev M. I. 2008. High resolution ^{26}Al-^{26}Mg chronometry of CAIs from the Allende meteorite (abstract #1999). 39th Lunar and Planetary Science Conference. CD-ROM.

Kita N. T. and Ushikubo T. 2012. Evolution of protoplanetary disk inferred from ^{26}Al chronology of individual chondrules. *Meteoritics & Planetary Science* 47:1108–1119.

Kita N. T., Nagahara H., Togashi S., and Morishita Y. 2000. A short duration of chondrule formation in the solar nebula: Evidence from ^{26}Al in Semarkona ferromagnesian chondrules. *Geochimica et Cosmochimica Acta* 64:3913–3922.

Kita N. T., Huss G. R., Tachibana S., Amelin Y., Nyquist L. E., and Hutcheon I. D. 2005. Constraints on the origin of chondrules and CAIs from short-lived and long-lived radionuclides. In *Chondrites and the protoplanetary disk*, edited by Krot A. N., Scott E. R. D., and Reipurth B. ASP Conference Series, vol. 341. San Francisco, California: Astronomical Society of the Pacific. pp. 558–587.

Kita N. T., Nagahara H., Tachibana S., Tomomura S., Spicuzza M. J., Fournelle J. H., and Valley J. W. 2010. High precision SIMS oxygen three isotope study of chondrules in LL3 chondrites: Role of ambient gas during chondrule formation. *Geochimica et Cosmochimica Acta* 74:6610–6635.

Kita N. T., Ushikubo T, Knight K. B., Mendybaev R. A., Davis A. M., Richter F. M., and Fournelle J. H. 2012. Internal ^{26}Al-^{26}Mg isotope systematics of a type B CAI: Remelting of refractory precursor solids. *Geochimica et Cosmochimica Acta* 86:37–51.

Kleine T., Hans U., Irving A. J., and Bourdon B. 2012. Chronology of the angrite parent body and implications for core formation in protoplanets. *Geochimica et Cosmochimica Acta* 84:186–203.

Komatsu M., Krot A. N., Petaev M. I., Ulyanov A. A., Keil K., and Miyamoto M. 2001. Mineralogy and petrography of amoeboid olivine aggregates from the reduced CV3 chondrites Efremovka, Leoville and Vigarano: Products of nebular condensation and accretion. *Meteoritics & Planetary Science* 36:629–641.

Krot A. N., Petaev M. I., and Yurimoto H. 2004. Amoeboid olivine aggregates with low-Ca pyroxenes: A genetic link between refractory inclusions and chondrules? *Geochimica et Cosmochimica Acta* 68:1923–1941.

Krot A. N., Nagashima K., Bizzarro M., Huss G. R., Davis A. M., Meyer B. S., and Ulyanov A. A. 2008. Multiple generations of refractory inclusions in the metal-rich carbonaceous chondrites Acfer 182/214 and Isheyevo. *The Astrophysical Journal* 672:713–721.

Krot A. N., Amelin Y., Bland P., Ciesla F. J., Connelly J., Davis A. M., Huss G. R., Hutcheon I. D., Makide K., Nagashima K., Nyquist L. E., Russell S. S., Scott E. R. D., Thrane K., Yurimoto H., and Yin Q.-Z. 2009. Origin and chronology of chondritic components: A review. *Geochimica et Cosmochimica Acta* 73:4963–4997.

Krot A. N., Makide K., Nagashima K., Huss G. R., Ogliore R. C., Ciesla F. J., Yang L., Hellebrand E., and Gaidos E. 2012. Heterogeneous distribution of ^{26}Al at the birth of the solar system: Evidence from refractory grains and inclusions. *Meteoritics & Planetary Science* 47:1948–1979.

Kunihiro T., Rubin A. E., McKeegan K. D., and Wasson J. T. 2004. Initial Al-26/Al-27 in carbonaceous-chondrite chondrules: Too little Al-26 to melt asteroids. *Geochimica et Cosmochimica Acta* 68:2947–2957.

Kurahashi E., Kita N. T., Nagahara H., and Morishita Y. 2008a. Al-26-Mg-26 systematics of chondrules in a primitive CO chondrite. *Geochimica et Cosmochimica Acta* 72:3865–3882.

Kurahashi E., Kita N. T., Nagahara H., and Morishita Y. 2008b. Al-26-Mg-26 systematics and petrological study of chondrules in CR chondrites (abstract). *Geochimica et Cosmochimica Acta* 72:A504.

Larsen K. K., Trinquier A., Paton C., Schiller M., Wielandt D., Ivanova M. A., Connelly J. N., Nordlund Å., Krot A. N., and Bizzarro M. 2011. Evidence for magnesium

isotope heterogeneity in the solar protoplanetary disk. *The Astrophysical Journal Letters* 735:L37 (7pp).

Liu M.-C., McKeegan K. D., Goswami J. N., Marhas K. K., Sahijpal S., Ireland T. R., and Davis A. M. 2009. Isotopic records in CM hibonites: Implications for timescales of mixing of isotope reservoirs in the solar nebula. *Geochimica et Cosmochimica Acta* 73:5051–5079.

Liu M.-C., Chaussidon M., Göpel C., and Lee T. 2012. A heterogeneous solar nebula as sampled by CM hibonite grains. *Earth and Planetary Science Letters* 327:75–83.

Ludwig K. R. 2003. Isoplot 3.00. A geochronological toolkit for Microsoft Excel. *Berkeley Geochronology Center Special Publication* 4:1–72.

MacPherson G. J. and Davis A. M. 1993. A petrologic and ion microprobe study of a Vigarano type B refractory inclusion: Evolution by multiple stages of alteration and melting. *Geochimica et Cosmochimica Acta* 57:231–243.

MacPherson G. J., Davis A. M., and Zinner E. K. 1995. The distribution of aluminum-26 in the early solar system–A reappraisal. *Meteoritics* 30:365–386.

MacPherson G. J., Huss G. R., and Davis A. M. 2003. Extinct 10Be in Type A calcium-aluminum-rich inclusions from CV chondrites. *Geochimica et Cosmochimica Acta* 67:3165–3179.

MacPherson G. J., Bullock E. S., Jenny P. E., Kita N. T., Ushikubo T., Davis A. M., Wadhwa M., and Krot A. N. 2010. Early solar nebula condensates with canonical, not supracanonical, initial $^{26}Al/^{27}Al$ ratios. *The Astrophysical Journal* 711:L117–L121.

MacPherson G. J., Kita N. T., Ushikubo T., Bullock E. S., and Davis A. M. 2012. Well-resolved variations in the formation ages for Ca-Al-rich inclusions in the early solar system. *Earth and Planetary Science Letters* 331–332:43–54.

Makide K., Nagashima K., Krot A. N., Huss G. R., Hutcheon I. D., and Bischoff A. 2009. Oxygen- and magnesium-isotope compositions of calcium–aluminum-rich inclusions from CR2 carbonaceous chondrites. *Geochimica et Cosmochimica Acta* 73:5018–5050.

Makide K., Nagashima K., Krot A. N., Huss G. R., Ciesla F. J., Hellebrand E., Gaidos E., and Yang L. 2011. Heterogeneous distribution of ^{26}Al at the birth of the solar system. *The Astrophysical Journal Letter* 733:L31 (5pp).

McKeegan K. D., Chaussidon M., and Robert F. 2000. Incorporation of short-lived ^{10}Be in a calcium-aluminum–rich inclusion from the Allende meteorite. *Science* 289:1334–1337.

McKeegan K. D., Kallio A. P. A., Heber V. S., Jarzebinski G., Mao P. H., Coath C. D., Kunihiro T., Wiens R. C., Nordholt J. E., Moses R. W., Jr., Reisenfeld D. B., Jurewicz A. J. G., and Burnett D. S. 2011. The oxygen isotopic composition of the Sun inferred from captured solar wind. *Science* 332:1528–1532.

Nagashima K., Krot A. N., and Chaussidon M. 2007. Aluminum-magnesium isotope systematics of chondrules from CR chondrites (abstract). *Meteoritics & Planetary Science* 42:A115.

Nagashima K., Krot A. N., and Huss G. R. 2008. ^{26}Al in chondrules from CR carbonaceous chondrites (abstract #2224). 39th Lunar and Planetary Science Conference. CD-ROM.

Norris T. L., Gancarz A. J., Rokop D. J., and Thomas K. W. 1983. Half-life of ^{26}Al. *Journal of Geophysical Research* 88: B331–B333.

Nyquist L. E., Kleine T., Shih C.-Y., and Reese Y. D. 2009. The distribution of short-lived radioisotopes in the early solar system and the chronology of asteroid accretion, differentiation, and secondary mineralization. *Geochimica et Cosmochimica Acta* 73:5115–5136.

Palme H. and Jones A. 2003. Solar system abundances of the elements. In *Meteorites, comets, and planets*, edited by Davis A. M., vol. 1. Treatise on Geochemistry, edited by Holland H. D. and Turekian K. K. Oxford: Elsevier-Pergamon. pp. 41–61.

Podosek F. A., Zinner E. K., MacPherson G. J., Lundberg L. L., Brannon J. C., and Fahey A. J. 1991. Correlated study of initial $^{87}Sr/^{86}Sr$ and Al-Mg systematics and petrologic properties in a suite of refractory inclusions from the Allende meteorite. *Geochimica et Cosmochimica Acta* 55:1083–1110.

Russell W. A., Papanastassiou D. A., and Tombrello T. A. 1978. Ca isotope fractionation on the Earth and other solar system materials. *Geochimica et Cosmochimica Acta* 42:1075–1090.

Russell S. S., Huss G. R., Fahey A. J., Greenwood R. C., Hutchison R., and Wasserburg G. J. 1998. An isotopic and petrologic study of calcium-aluminum-rich inclusions from CO3 meteorites. *Geochimica et Cosmochimica Acta* 62:689–714.

Sahijpal S. and Goswami J. N. 1998. Refractory phases in primitive meteorites devoid of ^{26}Al and ^{41}Ca: Representative samples of first solar system solids? *The Astrophysical Journal* 509:L137–L140.

Schiller M., Handler M., and Baker J. A. 2010. High-precision Mg isotopic systematics of bulk chondrites. *Earth and Planetary Science Letters* 297:165–173.

Scott E. R. D. and Krot A. N. 2003. Chondrites and their components. In *Meteorites, comets, and planets*, edited by Davis A. M., vol. 1. Treatise on Geochemistry, edited by Holland H. D. and Turekian K. K. Oxford: Elsevier-Pergamon. pp. 143–200.

Scott E. R. D. and Krot A. N. 2005. Chondritic meteorites and the high-temperature nebular origins of their components. In *Chondrites and the protoplanetary disk*, edited by Krot A. N., Scott E. R. D., and Reipurth B. ASP Conference Series, vol. 341. San Francisco, California: Astronomical Society of the Pacific. pp. 15–53.

Shu F. H., Shang H., and Lee T. 1996. Toward an astrophysical theory of chondrites. *Science* 277:1475–1479.

Spivak-Birndorf L., Wadhwa M., and Janney P. E. 2009. ^{26}Al-^{26}Mg systematics in D'Orbigny and Sahara 99555 angrites: Implications for high-resolution chronology using extinct chronometers. *Geochimica et Cosmochimica Acta* 73:5202–5211.

Sugiura N. and Krot A. N. 2007. ^{26}Al-^{26}Mg systematics of Ca-Al-rich inclusions, amoeboid olivine aggregates and chondrules in Acfer 094 chondrite. *Meteoritics & Planetary Science* 42:1183–1197.

Thrane K., Bizzarro M., and Baker J. A. 2006. Extremely brief formation interval for refractory inclusions and uniform distribution of ^{26}Al in the early solar system. *The Astrophysical Journal* 646:L159–L162.

Trinquier A., Birck J. L., and Allègre C. J. 2007. Widespread Cr-54 heterogeneity in the inner solar system. *The Astrophysical Journal* 655:1179–1185.

Ushikubo T., Tenner T. J., Hiyagon H., and Kita N. T. 2011. Lifetime of ^{16}O-rich oxygen isotope reservoir in the solar nebula (abstract #9086). Workshop on Formation of the first solids in the solar system. November 7–9, 2011, Kauai, Hawai'i. LPI Contribution No. 1639.

Ushikubo T., Nakashima D., Kimura M., Tenner T. J., and Kita N. T. 2013. Contemporaneous formation of chondrules in distinct oxygen isotope reservoirs. *Geochimica et Cosmochimica Acta* 109:280–295.

Villeneuve J., Chaussidon M., and Libourel G. 2009. Homogeneous distribution of ^{26}Al in the solar system from the Mg isotopic composition of chondrules. *Science* 325:985–988.

Wadhwa M., Amelin Y., Bogdanovski O., Shukolyukov A., Lugmair G. W., and Janney P. 2009a. Ancient relative and absolute ages for a basaltic meteorite: Implications for timescales of planetesimal accretion and differentiation. *Geochimica et Cosmochimica Acta* 73:5189–5201.

Wadhwa M., Janney P. E., and Krot A. N. 2009b. Evidence of disturbance in the ^{26}Al-^{26}Mg systematics of the Efremovka E60 CAI: Implications for the high-resolution chronology of the early solar system (abstract #2495). 40th Lunar and Planetary Science Conference. CD-ROM.

Wasserburg G. J., Lee T., and Papanastassiou D. A. 1977. Correlated O and Mg isotopic anomalies in Allende inclusions: II magnesium. *Geophysical Research Letters* 4:299–302.

Wasserburg G. J., Wimpenny J., and Yin Q.-Z. 2012. Mg isotopic heterogeneity, Al-Mg isochrons, and canonical ^{26}Al/^{27}Al in the early solar system. *Meteoritics & Planetary Science* 47:1980–1997.

Weber D., Zinner E., and Bischoff A. 1995. Trace element abundances and magnesium, calcium, and titanium isotopic compositions of grossite-containing inclusions from the carbonaceous chondrite Acfer 182. *Geochimica et Cosmochimica Acta* 59:803–823.

Wielandt D., Nagashima K., Krot A. N., Huss G. R., Ivanova M. A., and Bizzarro M. 2012. Evidence for multiple sources of ^{10}Be in the early solar system. *The Astrophysical Journal* 74:L25–L28.

Williams J. P. and Cieza L. A. 2011. Protoplanetary disks and their evolution. *Annual Review of Astronomy and Astrophysics* 49:67–117.

Wilson L., Goodrich C. A., and Van Orman J. A. 2008. Thermal evolution and physics of melt extraction on the ureilite parent body. *Geochimica et Cosmochimica Acta* 72:6154–6176.

Yang L. and Ciesla F. J. 2012. The effects of disk building on the distributions of refractory materials in the solar nebula. *Meteoritics & Planetary Science* 47:99–119.

Yin Q.-Z., Yamashita K., Yamakawa A., Jacobsen B., Ebel D., Hutcheon I. D., and Nakamura E. 2009. ^{53}Mn-^{53}Cr evidence for Allende chondrule formation at 4567.6 Ma. *Geochimica et Cosmochimica Acta* 73:A1484.

Yurimoto H., Krot A. N., Choi B.-G., Aléon J., Kunihiro T., and Brearley A. J. 2008. Oxygen isotopes of chondritic components. In *Oxygen in the solar system*, edited by MacPherson G. J., Mittlefehldt D. W., Jones J. H., Simon S. B., Papike J. J., and Mackwell S. Reviews in Mineralogy and Geochemistry, vol. 68. Washington, D.C.: Mineralogical Society of America. pp. 141–186.

APPENDIX

MASS-DEPENDENT FRACTIONATION LAWS

Due to the large range of mass-dependent magnesium isotope fractionations among CV CAIs, the δ^{26}Mg* values used in constructing the bulk CAI ^{26}Al-^{26}Mg regression line (isochron) must be corrected for mass-dependent fractionation to obtain real high-precision measurements (reproducible to better than 5 to 50 ppm). Here, we describe basic formulation of magnesium isotope systems that are used for ^{26}Al-^{26}Mg chronology and evaluate effects of mass fractionation correction schemes on the isochron regression.

Magnesium isotope ratios (^{25}Mg/^{24}Mg and ^{26}Mg/^{24}Mg) are described as δ^{25}Mg and δ^{26}Mg that are relative difference from those of the isotope reference material (DSM3) in the unit of parts in thousands (‰).

$$\delta^{25}\mathrm{Mg} = \left[\left(^{25}\mathrm{Mg}/^{24}\mathrm{Mg}\right)/\left(^{25}\mathrm{Mg}/^{24}\mathrm{Mg}\right)_{\mathrm{DSM3}} - 1\right] \times 1000 \quad \text{(A1)}$$

$$\delta^{26}\mathrm{Mg} = \left[\left(^{26}\mathrm{Mg}/^{24}\mathrm{Mg}\right)/\left(^{26}\mathrm{Mg}/^{24}\mathrm{Mg}\right)_{\mathrm{DSM3}} - 1\right] \times 1000 \quad \text{(A2)}$$

The magnesium isotope ratios of the international standard DSM3 are very close to those of CI chondrites (Galy et al. 2003) and are presumably similar to those of absolute measurements of Catanzaro et al. (1966) with the values ^{25}Mg/^{24}Mg = 0.12663 ± 0.00013 and ^{26}Mg/^{24}Mg = 0.13932 ± 0.00026.

Here, we consider a group of objects that formed in the early solar system with common magnesium isotope ratios and they experienced processes that involved mass-dependent fractionation at the variable degrees. The δ^{25}Mg and δ^{26}Mg values of individual objects are described by power function with an exponent β as a mass-dependent term.

$$\left[1 + \frac{\delta^{26}\mathrm{Mg}}{1000}\right] = \left[1 + \frac{\delta^{25}\mathrm{Mg}}{1000}\right]^{1/\beta} \times \left[1 + \frac{(\delta^{26}\mathrm{Mg}^*)_0}{1000}\right], \quad \text{(A3)}$$

where $(\delta^{26}\mathrm{Mg}^*)_0$ is the mass-independent fractionation of the common isotope reservoir relative to DSM3. If these objects contained ^{26}Al with initial ratios of $(^{26}\mathrm{Al}/^{27}\mathrm{Al})_0$ at their formation, addition of radiogenic ^{26}Mg* increases δ^{26}Mg after the complete decay of ^{26}Al as follows.

$$\left[1 + \frac{\delta^{26}\mathrm{Mg}}{1000}\right] = \left[1 + \frac{\delta^{25}\mathrm{Mg}}{1000}\right]^{1/\beta} \times \left[1 + \frac{(\delta^{26}\mathrm{Mg}^*)_0}{1000}\right] + \frac{(^{26}\mathrm{Al}/^{27}\mathrm{Al})_0 \times (^{27}\mathrm{Al}/^{24}\mathrm{Mg})}{(^{26}\mathrm{Mg}/^{24}\mathrm{Mg})_{\mathrm{DSM3}}} \quad \text{(A4)}$$

In the case that the $(\delta^{26}Mg^*)_0$ is very close to 0 (e.g., $\leq \pm 0.1‰$) and the range of $\delta^{25}Mg$ value is within those observed among non-FUN CAIs ($-2‰$ to $+10‰$), Equation A4 is approximated by

$$\left[1+\frac{\delta^{26}Mg}{1000}\right]=\left[1+\frac{\delta^{25}Mg}{1000}\right]^{1/\beta}+\frac{(\delta^{26}Mg^*)_0}{1000}+\frac{(^{26}Al/^{27}Al)_0\times(^{27}Al/^{24}Mg)}{(^{26}Mg/^{24}Mg)_{DSM3}} \quad (A5)$$

Equation A5 is modified to the formula using $\delta^{26}Mg^*$ to represent the ^{26}Al-^{26}Mg isochron diagram, in which the slope of isochron is a function of initial $(^{26}Al/^{27}Al)_0$.

$$\delta^{26}Mg^*=(\delta^{26}Mg^*)_0+\frac{(^{26}Al/^{27}Al)_0\times 1000}{(^{26}Mg/^{24}Mg)_{DSM3}}\times(^{27}Al/^{24}Mg), \quad (A6)$$

where $\delta^{26}Mg^*$ is defined as

$$\delta^{26}Mg^*=\left[\left(1+\frac{\delta^{26}Mg}{1000}\right)-\left(1+\frac{\delta^{25}Mg}{1000}\right)^{1/\beta}\right]\times 1000 \quad (A7)$$

There are two different values of β in Equation A7 that have been used to correct natural mass-dependent isotope fractionation of magnesium in meteoritic samples. One is $\beta = 0.511$, which is called the exponential law (Russell et al. 1978) that has become the most commonly used for correcting for both instrumental (thermal ionization, ICP-MS, and SIMS) and natural mass fractionation effects to obtain high-precision isotope ratios. It was first used for ^{26}Al-^{26}Mg chronology of bulk CAIs by Bizzarro et al. (2004). Following this work, later bulk CAI isochron data obtained by MC-ICP-MS solution measurements have been reduced using the exponential law (e.g., B. Jacobsen et al. 2008). Another is $\beta = 0.514$ according to the evaporation experiments of CAI-like melt (Davis et al. 2005), which has been used for several internal isochron studies of igneous CAIs (e.g., Bouvier and Wadhwa 2010; Kita et al. 2012).

The choice of β values would change individual data points on the isochron diagram by more than 0.05‰ (Fig. 1A), which is beyond the precision of magnesium isotope measurements. The $\delta^{26}Mg^*$ values calculated using β approximately 0.514 would increase for CAIs with heavy isotope enrichments (typical for coarse-grained CAIs) and decrease for CAIs with light isotope enrichments (typical for fine-grained CAIs) compared with those using $\beta = 0.511$. B. Jacobsen et al. (2008) reported that the slope and the intercept of the bulk CV CAI isochron change from $(^{26}Al/^{27}Al)_0 = (5.23 \pm 0.13) \times 10^{-5}$ and $(\delta^{26}Mg^*)_0 = -0.040 \pm 0.029‰$ for $\beta = 0.511$ to $(^{26}Al/^{27}Al)_0 = (5.19 \pm 0.12) \times 10^{-5}$ and $(\delta^{26}Mg^*)_0 = -0.001 \pm 0.031‰$ for $\beta = 0.514$. These two regression lines agree within the uncertainties. In the case of data from Larsen et al. (2011) with more improved analytical precisions ($\pm 0.0025‰$ in $\delta^{26}Mg^*$ values), five CAI data points are exactly on the regression line within their analytical uncertainties, while their $\delta^{26}Mg^*$ values range from 0.99‰ to 1.24‰ and $\delta^{25}Mg$ values range from $-2.4‰$ to $+12‰$. By using $\beta = 0.514$ for the mass fractionation corrections, these data shift both above and below the regression line determined with $\beta = 0.511$ and do not plot on a single line within their analytical uncertainties.

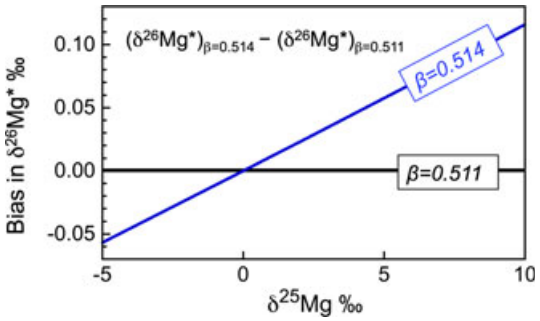

Fig. A1. Bias in excess $\delta^{26}Mg^*$ resulting from two different mass-dependent fractionation corrections. The excess $\delta^{26}Mg^*$ values are calculated by using Equation A1 with $\beta = 0.514$ (evaporation experiments) and $\beta = 0.511$ (exponential law) as a function of stable isotope mass fractionation ($\delta^{25}Mg$). The figure shows the bias in excess $\delta^{26}Mg^*$ for $\beta = 0.514$ relative to the value calculated for $\beta = 0.511$. The $\delta^{25}Mg$ values reported for CAIs are typically from $-2‰$ to $+10‰$, which may result in significant systematic errors (up to 0.1‰) for the magnesium isotope analyses.

Improper assignment of β would be a serious problem for high-precision ^{26}Al-^{26}Mg data. We should note that the β from melt evaporation experiment may not be relevant to fine-grained CAIs that did not experience melting. B. Jacobsen et al. (2008) and Wasserburg et al. (2012) argue that CAI data corrected with $\beta = 0.511$ show better linearity than those with $\beta = 0.514$, according to MSWD (mean square weighted deviations) of isochron regression, which is a measure of ratio of observed scatter of points (from best fit line, i.e., natural uncertainty) to the expected scatter (from assigned error and error correlation, i.e., analytical uncertainty). These statistical arguments would support

Table A1. Internal isochron regressions of CV3 CAIs with different β factors[a].

		β = 0.514			β = 0.511				
Inclusions		$(^{26}Al/^{27}Al)_0$ $\times 10^{-5}$	$(\delta^{26}Mg^*)_0$ ‰	MSWD	$(^{26}Al/^{27}Al)_0$ $\times 10^{-5}$	$(\delta^{26}Mg^*)_0$ ‰	MSWD	Ref.[b]	β[c]
Vigarano F8	FTA	5.29 ± 0.28	−0.07 ± 0.11	1.9	5.27 ± 0.26	−0.06 ± 0.10	1.7	[1]	0.514
Leoville 3536	FTA	5.27 ± 0.17	0.02 ± 0.06	1.3	5.25 ± 0.17	0.05 ± 0.06	1.3	[2]	0.514
Vigarano F5	AOA	5.13 ± 0.11	−0.020 ± 0.015	1.0	4.94 ± 0.11	0.010 ± 0.015	1.3	[1]	0.514
Vigarano F9	CTA	5.17 ± 0.31	0.0 ± 0.15	4.3	5.22 ± 0.32	−0.11 ± 0.16	4.6	[1]	0.514
Allende A44A	B	5.13 ± 0.21	0.035 ± 0.068	4.4	5.06 ± 0.15	0.010 ± 0.052	1.8	[3]	0.511
NWA 2364	B	5.03 ± 0.26	0.02 ± 0.06	1.2	5.02 ± 0.36	−0.02 ± 0.08	1.7	[4]	0.514
Leoville 3535-1	B	5.002 ± 0.065	0.06 ± 0.08	5.4	5.002 ± 0.065	0.00 ± 0.08	5.6	[5]	0.514
Allende AJEF	B	5.01 ± 0.20	−0.011 ± 0.046	0.9	4.96 ± 0.25	−0.018 ± 0.061	0.6	[3]	0.511
Vigarano F1	B	4.66 ± 0.17	0.18 ± 0.06	4.8	4.74 ± 0.17	0.10 ± 0.06	4.8	[1]	0.514
Allende A43	B	4.39 ± 0.40	0.145 ± 0.077	1.2	4.47 ± 0.42	0.098 ± 0.077	1.1	[3]	0.511
Vigarano F6	CTA	4.24 ± 0.36	0.09 ± 0.17	3.8	4.32 ± 0.35	0.02 ± 0.16	3.6	[1]	0.514
Vigarano F4	C	2.8 ± 0.8	0.52 ± 0.12	8.1	2.7 ± 0.8	0.50 ± 0.12	8.1	[1]	0.514
	rel A	4.78 ± 0.31	0.24 ± 0.24	12	4.76 ± 0.29	0.21 ± 0.23	12		

[a]For Allende type B CAI data, isochron regression parameters for two β values are from [3]. For other data, regression parameters were reported by using β = 0.514 in the literature. Therefore, $\delta^{26}Mg^*$ values are recalculated for β = 0.511 from the reported $\delta^{25}Mg$ and $\delta^{26}Mg^*$ values and isochron regression parameters for β = 0.511 are obtained using ISOPLOT program (Ludwig 2003).

[b][1] MacPherson et al. 2012; [2] MacPherson et al. 2010; [3] B. Jacobsen et al. 2008; [4] Bouvier and Wadhwa 2010; [5] Kita et al. 2012.

[c]β values used in the literature.

β = 0.511 for CAIs, although there is no reason to assume that data from natural CAIs should show isochrons without a significant scatter.

For the internal isochron of individual CAIs, which generally show nearly constant $\delta^{25}Mg$ values, the slope of the isochron is insensitive to β values, but intercept $(\delta^{26}Mg^*)_0$ would be biased. In Table 1A, we compare the results of internal isochron regression of CAIs by using β factors of 0.514 and 0.511. None of the regression lines using two β values differ beyond the uncertainty of the isochron fits. In most cases, nominal values of $(^{26}Al/^{27}Al)_0$ agree within 2%.